Quaternary Science Reviews 300 (2023) 107898

Contents lists available at ScienceDirect

Quaternary Science Reviews

journal homepage: www.elsevier.com/locate/quascirev

Plants, people and fire: Phytolith and FTIR analyses of the post-Howiesons Poort occupations at Border Cave (KwaZulu-Natal, South Africa)

Irene Esteban [a, b, c, *], Dominic Stratford [d], Christine Sievers [d], Paloma de la Peña [b, e, f], Guilhem Mauran [b, g], Lucinda Backwell [b, h, i], Francesco d'Errico [g, j], Lyn Wadley [b]

[a] ERAAUB, Dept. de Història i Arqueologia, and Institut d'Arqueologia de la Universitat de Barcelona, Carrer de Montalegre 6-8, 08001, Universitat de Barcelona, Barcelona, Spain
[b] Evolutionary Studies Institute, University of the Witwatersrand, Private Bag 3, WITS, 2050, Johannesburg, South Africa
[c] African Centre for Coastal Palaeoscience, Nelson Mandela University, Port Elizabeth, South Africa
[d] Department of Archaeology, School of Geography, Archaeology and Environmental Studies, University of the Witwatersrand, Private Bag 3, WITS, 2050, South Africa
[e] Departamento de Prehistoria y Arqueología, Universidad de Granada, Campus Universitario de Cartuja s/n, 18071, Granada, Spain
[f] McDonald Institute for Archaeological Research, University of Cambridge, Downing Street, Cambridge, CB2 3ER, United Kingdom
[g] Univ. Bordeaux, UMR, 5199, CNRS de la Préhistoire à l'Actuel: Culture, Environnement, et Anthropologie (PACEA), Université de Bordeaux, Allée Geoffroy Saint Hilaire, CS 50023, F - 33615, Pessac CEDEX, Talence, France
[h] Grupo de Investigación en Arqueología Andina (ARQAND-CONICET), Facultad de Ciencias Naturales e Instituto Miguel Lillo, Universidad Nacional de Tucumán, Calle Miguel Lillo 205, San Miguel de Tucumán, Tucumán, T4000, Argentina
[i] Centre of Exploration for the Deep Human Journey, University of the Witwatersrand, Private Bag 3, WITS, 2050, South Africa
[j] Centre for Early Sapiens Behaviour, Øysteinsgate 3, Postboks 7805, 5020, University of Bergen, Norway

ARTICLE INFO

Article history:
Received 31 May 2022
Received in revised form
11 November 2022
Accepted 27 November 2022
Available online xxx

Handling Editor: Donatella Magri

Keywords:
Phytoliths
FTIR
Taphonomy
Pyrotechnology
Bedding
Middle Stone Age
South Africa

ABSTRACT

Border Cave is a well-known South African Middle and Early Later Stone Age site located in KwaZulu-Natal. The site has exceptional plant preservation, unparalleled in the African Middle Stone Age archaeological record. This study focuses on the phytolith and FTIR analysis of two Members (2 BS and 2 WA) of the under-documented post-Howiesons Poort occupations dating to ~60 ka. These members contain complex successions of vertically overlapping, interdigitating light brown sediments, plant bedding and combustion features of various sizes. The complexity and distinctiveness of these deposits provide an excellent opportunity for the study of plant exploitation strategies and their associated human behaviour. Our taphonomic assessment inferred, through the variability of phytolith properties and minerals composing archaeological layers, that specific occupations suffered more physical weathering than others, for example in the form of trampling. The preservation of fragile and highly soluble phytoliths (eudicot leaf phytoliths) and the high frequencies of articulated phytoliths indicates that some bedding deposits experienced little disturbance after their deposition. Not all bedding layers dating to ~60 ka show, from a phytolith perspective, the same plant composition, which could be explained in terms of changes in human preference for the use of plants over time to construct bedding or because distinct types of living floors are represented. Finally, the systematic application of phytoliths and FTIR to the complex archaeological sequence of Border Cave confirm these analyses can be used in the future to identify bedding deposits not visible to the naked eye, and behavioural patterns obscured by diagenetic or biased processes during sampling.

1. Introduction

Plants are one of the most widely used natural resources of South African indigenous communities for food and drink, medicine and beauty, tools, and crafts (van Wyk and Gericke, 2000; van

* Corresponding author. ERAAUB, Dept. de Història i Arqueologia, and Institut d'Arqueologia de la Universitat de Barcelona, Carrer de Montalegre 6-8, 08001, Universitat de Barcelona, Barcelona, Spain.
E-mail address: irene.esteban@ub.edu (I. Esteban).

https://doi.org/10.1016/j.quascirev.2022.107898

Wyk, 2008; Mogale et al., 2019). Plants constitute the basis of their diets, and although cultivated plants may dominate, the use of wild plants is still widespread (van Wyk and Gericke, 2000; de Vynck et al., 2016; Mayori, 2017). Wood remains an important energy source to make fires for cooking, lighting, and heating in South African rural households (van Wyk and Gericke, 2000; Shackleton et al., 2022), and is the primary resource for southern African hunter-gatherers (Wiessner, 2014). Plants are also widely used to construct shelters or create comfortable spaces to sleep, rest and work (van Wyk and Gericke, 2000), and to create various tools to hunt, fish and store, and transport foods and all sorts of goods (van Wyk and Gericke, 2000; Mogale et al., 2019). The cultural material signals that can thus be obtained from the study of plants are broad, and the study of botanical remains from the southern African archaeological record has been crucial in reconstructing many of the daily activities performed by past hunter-gatherer societies (e.g. Deacon, 1993; d'Errico et al., 2012; Bentsen, 2014; Wadley et al., 2020a, 2020b).

Archaeobotanical evidence has also been used to propose complex cultural behaviours of South African Stone Age populations (Deacon, 1993; Wadley et al., 2011, 2020a, 2020b), such as during the post-Howiesons Poort (post-HP) of the Middle Stone Age (MSA). The post-HP dates from around 60 ka to 25 ka years ago in southern Africa (Wadley, 2015). Mackay et al. (2014) describe post-HP assemblages as more heterogeneous than other MSA industries. According to Wadley (2015), the term post-HP is a 'catch-all' category for highly variable lithic assemblages across the subcontinent. These assemblages usually are flake-based and sometimes they have a notable representation of unifacial points (Wadley, 2015). Based on the lithic assemblage from Sibudu Cave, Conard et al. (2012) and Will (2019) proposed a new technocomplex, 'the Sibudan' (~58 ka), made from local raw materials using multiple reduction methods including *Levallois*, discoid, platform, and bipolar knapping to produce predominantly convergent flakes and blades. These traits have recently been identified in Member 2 BS and part of 2 WA at Border Cave (de la Peña et al., 2022; Timbrell et al., 2022). Some researchers consider that the post-HP is represented in the South African archaeological record by a decrease in lithic technological complexity (e.g. Villa et al., 2005; McCall, 2007, but see Lombard and Parsons, 2011; Dusseldorp, 2014) attributing the gradual changes to a progressive shift in the technical system that entailed the development of innovations in behavioural domains, such as bone tools, hafting, adhesives, ornaments or wooden tools. Others suggest that this was a period of change in economic strategies, patterns of mobility, and social organization that were driven by changes in global climate, demography and/or resource structure (Lombard and Parsons, 2011; Dusseldorp, 2014; Will, 2019).

Archaeobotanical research results for the post-HP at Sibudu include evidence of stability in the construction of combustion features in contrast to the changes observed in other cultural aspects (Wadley, 2012) and the deliberate construction and placement of plant bedding (Goldberg et al., 2009; Wadley et al., 2011). At Pinnacle Point 5–6, there is evidence for the targeted collection of dry firewood to support consistent heat treatment of silcrete to produce the bladelet and microlithic technology recorded (Esteban et al., 2018). The latter comes from phytolith and Fourier Transform Infrared Spectroscopy (FTIR) data, two techniques that in South Africa have helped researchers better understand site formation processes (Schiegl and Conard, 2006; Esteban et al., 2020), the fuel used to make fires and their intensity and maintenance (Esteban et al., 2018), and identify changes in fuel in relation to site occupation patterns during the MSA (Schiegl et al., 2004; Schiegl and Conard, 2006; Esteban et al., 2018). Phytoliths and FTIR analyses, together with other botanical studies and analytical techniques, have also been applied to the site of Border Cave, demonstrating the use of several species of Panicoideae grasses and aromatic leaves to construct bedding that was deliberately placed on top of ash to repel insects and other pests 227 ka years ago (Wadley et al., 2020b).

The work presented here builds on this latter study to investigate further the use of plants at Border Cave during the poorly understood post-HP period. We focus on the complex succession of distinct vertically and laterally overlapping combustion features, bedding layers and light brown deposits in units 2 BS.LR C to 2 WA (Fig. 1), which date to between ~ 60 ka and ~50 ka years ago. The study of these deposits through phytolith and FTIR analysis provides an excellent opportunity to glean information about plant exploitation strategies, with special emphasis on bedding practices, pyrotechnology and site occupation patterns. This work aims to expand the phytolith and mineralogical study to analyse these deposits at a micro-scale to decipher their taphonomic histories and reconstruct plant uses, while providing support for ongoing multiscale, multiproxy geoarchaeological research (see Stratford et al., 2022).

1.1. Background to the site

Border Cave is an MSA site located on the border between South Africa and eSwatini (formerly Swaziland), about 90 km inland from the Indian Ocean (Fig. 1). The site is situated in the remote Lebombo mountains of KwaZulu-Natal province, facing west from a well-wooded, steep cliff above the eSwatini lowveld. The shelter is 50 m wide and 35 m long. It formed approximately 182.1 ± 2.9 mya (Riley et al., 2004) in the Lower Jurassic felsic extrusive Jozini Formation (Lebombo Group), generally represented by a variety of igneous rhyolitic facies with interbedded sandstones (Butzer et al., 1978). Two volcaniclastic facies of the Jozini Formation are exposed in the cave: a clast- and a matrix-supported breccia. The cave formed through the preferential weathering of the less lithified components in these facies (Cooke et al., 1945; Backwell et al., 2018). The mountains experience frequent morning mists and summer rainfall varying between 550 and 1000 mm with an average of 781 mm per annum. Marked differences in elevation, soils, and moisture availability have produced a mosaic of vegetation types within 5 km of the cave (Butzer et al., 1978). Lowveld (Zululand Lowveld) and riverine vegetation (Lowveld Riverine Forests, among other riparian flora) occur in the lowlands of eSwatini which can be viewed from the cave. Open bushveld (Northern and Southern Lebombo Bushveld) and tall, sour and wiry grasslands often dotted with low bushes and solitary savanna trees (Lebombo Summit Sourveld) also occur in the Border Cave region (Rutherford et al., 2006). A botanical survey of the area was conducted by Anderson (1978) and the results of a recent survey are presented in Backwell et al. (2018).

The site contains a long sedimentary sequence of cultural material with pulses of occupation spanning the last 227,000 years (Backwell et al., 2018, 2022) that have yielded MSA human remains (Backwell et al., 2018; Beaudet et al., 2022), the earliest evidence of a personal ornament associated with a burial (d'Errico and Backwell, 2016), and what Beaumont called Early Later Stone Age (ELSA) technology (Beaumont and Vogel, 1972; Vogel and Beaumont, 1972) with numerous examples of cultural innovation (d'Errico et al., 2012; Villa et al., 2012a, b). The site also has exceptional plant and organic preservation, unparalleled in the African MSA archaeological record (Backwell et al., 2018, 2022)..

The sedimentary sequence of Border Cave formed through a combination of geological and anthropogenic processes, which were stratigraphically divided by Beaumont (1973, 1978) and Butzer et al. (1978) into alternating Brown Sand (BS) and White Ash

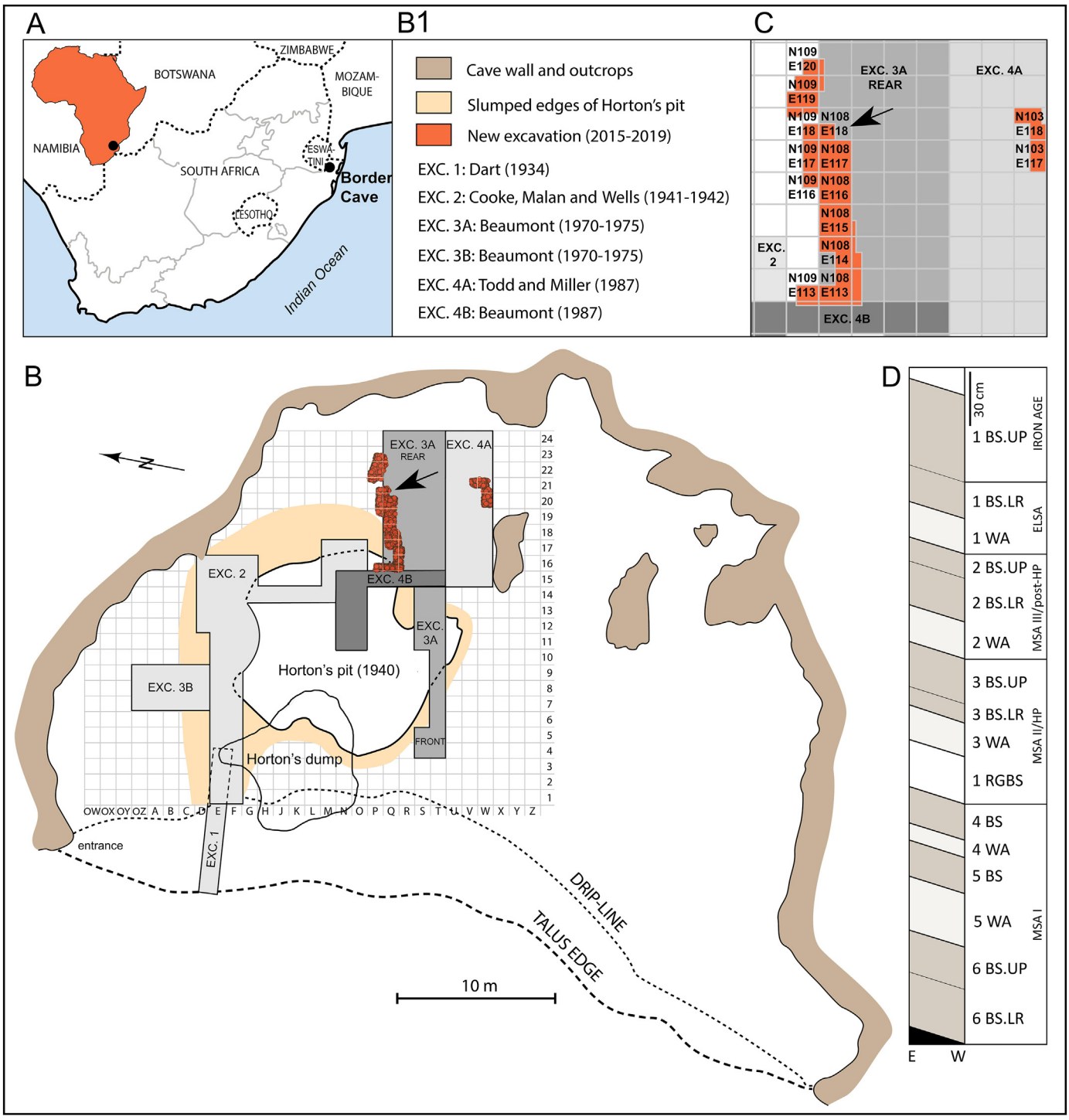

Fig. 1. Location and site plan of Border Cave. A. Map showing the location of the site in South Africa. **B.** Site plan showing the position of the various excavations conducted from 1934 to 2019. The grid is the original one established by Cooke et al., 1945. The orange overlay shows the areas excavated by us from 2015 to 2019 along the North wall of excavation (EXC.) 3 A rear and South wall of EXC. 4 A. The arrow points to where the phytolith samples were taken for this study. **B1.** Key to site plan. **C.** Close-up of the areas excavated by us showing the square names according to North and East lines. The arrow indicates where the phytolith samples were taken in square N109 E118. **D.** Stratigraphic members and associated cultural attributions according to Beaumont et al. (1992). The alternating colours denote Brown Sand (darker grey) and White Ash (lighter grey) members, and the sloped dividing lines represent the dip of the deposit. (For interpretation of the references to colour in this figure legend, the reader is referred to the Web version of this article.)

(WA) members based on whether the stratified sedimentary units were predominantly white from accumulated ash (WA members) or whether they were mostly brown sand (BS members). In 2015, Backwell, Wadley and d'Errico renewed excavations at the site and these new excavations retain the general stratigraphic framework nomenclature of Beaumont. Their strategy focuses on sampling small areas of the sequence exposed by Beaumont when he opened a large trench that exposed the youngest to the oldest deposits (Exc. 3 A Rear in Fig. 1B). The samples studied here come from these newly excavated deposits. Fig. 1D shows the stratigraphy of the

Table 1
List of the samples analysed in this study giving location, description and facies association as well as the main phytolith and mineralogical results and percentage of diatoms. Minerals are listed based on their relative concentration in sediments, from highest to lowest as roughly indicated by the relative peak heights in the infrared spectra. WM, weathered morphologies; C, calcite; Cl, clay minerals; Gy, gypsum; C.Ha, carbonate hydroxyapatite; Org. Mat, organic matter; Q, quartz; R, rhyolite. # Phytoliths, phytoliths counted with identifiable morphology. Phytolith concentration, phytoliths per gram of sediment (in million).

Sample Number	Member units	Layer	Sample description	Facies following Stratford et al., 2022	# Phytoliths	Phytolith concentration	% Diatoms	% WM	% Articulated phytoliths	# Morphotypes	% Fragile morphotypes	Compound composition
S.22	2 BS.LR C	Dark Greyish Brown to Orange Silty	Light brown	Facies I.I - Massive clast-poor silty sand	260	10.4	7.5	0	37.3	37	25.0	Cl, Gy, C.Ha, Org. Mat., C
S.21	2 BS.LR C	Dark Greyish Brown	Black	Facies IV - Massive charcoal	309	10.1	4.3	0.6	39.2	36	9.1	Cl, C.Ha, Q, Gy, Org. Mat.
S.69	2 BS.LR C	Dark Greyish Brown	Light brown	Facies VI - Homogeneous anthropogenic components	281	5.5	6.6	1.1	28.5	37	10.0	Cl, Q, C.Ha, Gy, Org. Mat.
S.68	2 BS.LR C	Grass Mat 1 b. c	Black	Facies VI - Homogeneous anthropogenic components, with high proportion of charcoal – potentially post-depositionally altered Facies III	295	10.2	3.6	1	56.3	34	5.4	Cl, Gy, C.Ha, Q, Org. Mat.
S.67	2 BS.LR C	Grass Mat 1 and 2	Light brown	Facies VI - Homogeneous anthropogenic components	260	13.7	8.1	0	21.9	41	13.5	Cl, Q, Gy, Org. Mat., R, C.Ha
S.66	2 BS.LR C	Grass Mat 1 b. c	Bedding	Facies V - Laminated organic matter	390	10.1	7.1	0	60.8	34	50.3	Cl, Gy, C.Ha, Q, Org. Mat.
S.20	2 BS.LR C	Grass Mat 1 and 2	Light brown	Facies VII – Homogeneous (with stratified) anthropogenic components	299	14.8	2.2	2	58.5	35	43.1	Cl, Q, C.Ha, Org. Mat., Gy, C
S.19	2 BS.LR C	Grass Mat with bone	Bedding	Facies V - Laminated organic matter	420	14.5	1.4	0	88.6	30	44.3	Cl, Gy, C.Ha, Q, C, Org. Mat.
S.18	2 W A.UP	White Ash	Ash	Facies III – Ash	87	14.7	0.5	76.1	62.1	22	14.9	C, Cl, C.Ha, Q
S.17	2 W A.UP	Light Reddish Brown	Rubified	Facies I - Massive Sands or VI - Homogeneous anthropogenic components	261	14.4	17.4	0	50.2	33	5.8	Cl, Q, Gy, C.Ha, C
S.16	2 W A.UP	Black	Black	Facies IV - Massive charcoal	258	6.3	8.1	1.9	37.6	36	12.8	Gy, Cl, C.Ha
S.15	2 W A.UP	Light Reddish Brown	Black	Facies VI - Homogeneous anthropogenic components	254	7.6	7.6	0.4	46.1	29	8.7	Cl, Q, R, C
S.14	2 W A.LR	Contact between Dark Brown Dijon and Dark Yellowish Brown Devo	Light brown	Facies I - Massive sands	269	6.1	10.5	1.5	34.9	33	8.6	Cl, Q, R, C, Org, mat,
S.13	2 W A.LR	Dark Brown Dijon	Bedding	Facies V - Laminated organic matter	301	5.5	2.9	0.7	43.2	34	16.9	Cl, Q, R, C
S.12	2 W A.LR	Dark Brown Dijon	Black	Facies VI - Homogeneous anthropogenic components (right on the edge of a pocket of Facies IV - Massive charcoal)	223	1.7	6.3	0	39.9	31	17.0	Cl, Q, R, C
S.10	2 W A.LR	Dark Yellowish Brown Dino	Light brown	Facies I - Massive sands	216	6.6	6.4	1.4	24.1	33	9.3	Cl, Q, Org. Mat., Gy, R
S.11	2 W A.LR	Dark Yellowish Brown Dossy	Black	Facies IV - Massive charcoal	332	5.1	3.8	0.3	61.5	34	40.1	Cl, Q, R
S.9	2 W A.LR	Dark Yellowish Brown Dossy	Light brown	Facies I - Massive sands	227	4.6	5.2	4.6	29.1	34	16.7	Cl, Q, Org. Mat., Gy, R
Modern soil outside the cave entrance			Control sample	Grassy area surrounded by various herbs and eudicot trees.	245	3.5	32.6	2.4	9.5	28	4.5	Cl, Hum. Acid, Q, Org. Mat.
Site's surface			Control sample	Overburden deposits with lots of bat guano	80	0.8	0	9.1	7.5	18	8.8	Unidentified organic matter and polysaccharides, silicates, Gy

Table 2
Non-parametric Spearman's correlation analysis measuring phytolith variables to evaluate taphonomic processes affecting the phytolith assemblage at Border Cave. Significant *p* values (<0.05) in bold. WM: weathered morphologies.

Phytolith concentration	Taphonomic indicator	ρ Spearman	Prob > |ρ|
Archaeological and control samples			
Phytoliths per gram of sediment	% WM	−0,2644	0,2599
Phytoliths per gram of sediment	% Fragile morphotypes	0,2165	0,3591
Phytoliths per gram of sediment	% Articulated phytoliths	0,5459	**0,0128**
Phytoliths per gram of sediment	Total number of morphotypes	0,2225	0,3458
% Articulated phytoliths	WM	−0,3086	0,1856
# Morphotypes	WM	−0,2982	0,2016
# Morphotypes	% Articulated phytoliths	−0,1093	0,6463
% Fragile morphotypes	WM	−0,3292	0,1564
% Fragile morphotypes	% Articulated phytoliths	0,4797	**0,0323**
% Fragile morphotypes	# Morphotypes	0,2703	0,2490
Archaeological samples only			
Phytoliths per gram of sediment	% WM	−0.0915	0.7182
Phytoliths per gram of sediment	% Fragile morphotypes	0.0506	0.8421
Phytoliths per gram of sediment	% Articulated phytoliths	0.3953	0.1045
Phytoliths per gram of sediment	Total number of morphotypes	−0.0293	0.9081
% Articulated phytoliths	WM	−0.1282	0.6121
# Morphotypes	WM	−0.0495	0.8452
# Morphotypes	% Articulated phytoliths	−0.4927	**0.0378**
% Fragile morphotypes	WM	−0.2292	0.3604
% Fragile morphotypes	% Articulated phytoliths	0.3808	0.1190
% Fragile morphotypes	# Morphotypes	0.0785	0.7570

members from 1 BS to 6 BS and their associated cultural attributions. The sedimentary deposit, particularly in the Brown Sand members, is dominated by sand-sized particles of fragmented rhyolite that decayed from the rhyolitic host rock, with variable subordinate contributions of sand deriving from the sandstone incorporated in the host rock facies. The most common anthropogenic features in WA and BS members are combustion features and plant bedding. However, these are more abundant in WA members (Backwell et al., 2018, 2022; Stratford et al., 2022).

The site has been thoroughly dated through electron spin resonance (Grün and Beaumont, 2001; Grün et al., 2003; Millard, 2006), amino acid racemisation (Miller et al., 1999), and radiocarbon methods (Vogel and Beaumont, 1972; Butzer et al., 1978; Beaumont, 1980; Vogel et al., 1986; Beaumont et al., 1992; Bird et al., 2003; d'Errico et al., 2012; Villa et al., 2012b; Backwell et al., 2018). Some units have recently been re-dated by Tribolo et al. (2022) using the luminescence method to age feldspar grains in the sedimentary sequence. Their minimum and maximum age estimates and Bayesian model ages are in general agreement with those previously obtained. Dating information and associated lithic technological complexes are listed in Supplementary Online Material (SOM) 1, Table S1.

2. Materials and methods

2.1. Materials

Eighteen sediment samples were collected in November 2020 from discernible layers in Lower C unit of Member 2 BS (2 BS.LR C) and Upper and Lower units of Member 2 W A (2 W A.UP and 2 W A.LR) on the south-facing profile of excavation square N109 E118, which is one of our squares located on the north face of Beaumont's excavation 3 A rear (Fig. 2). 2 BS.LR C dates from 57.9 to 50.3 ka and layers from 2 W A date to 63.7 to 53.6 ka (ages indicate the Highest Posterior Density (HPD) at 95% of the Bayesian model age estimates of Tribolo et al. (2022). Sampling aimed to obtain a representation of sediments from a variety of types of deposits: the predominantly geogenic layers, which contain few anthropogenic artefacts and are light brown in colour; bedding layers that preserve plant material; and other distinctive layers such as black, white and reddish deposits, typically associated with combustion features. Two additional samples were also considered in this study as control samples, one from the vegetated area outside the cave entrance and one from the site's surface, which is an overburden layer with a lot of bat guano.

2.2. Methods

Phytolith extraction from the archaeological sediments was carried out at the Laboratory of Archaeology at the University of Barcelona (Spain)[1] following the rapid extraction procedure of Katz et al. (2010). Quantification of the total phytoliths per gram of sediment was based on the screening of 20 fields at 200x magnification following directives given by these authors, and concentrations are given per gram of sediment. The morphological identification of phytoliths was conducted at 400x magnification using an optical microscope (Zeiss Primostar 3) counting between 200 and 300 phytoliths. The International Code for Phytolith Nomenclature 2.0 (ICPN, Neumann et al., 2019) was followed to describe and name the phytoliths whenever possible (Table S2 in SOM 2). We also counted diatoms and sponge spicules, but taxonomic identifications of these were not made.

We investigated the degree of preservation of the phytolith assemblage by measuring the strength of association between the phytolith concentration (phytoliths per gram of sediment) and four taphonomic indicators [% weathered morphotypes, % delicate morphologies, % of articulated phytoliths (phytoliths in anatomical connection) and the total number of morphotypes identified] using Spearman's correlation coefficient analysis (Table 2). We further used the non-parametric Kruskal-Wallis test to explore the distribution of phytolith concentration, phytolith taphonomic indicators and phytolith morphotypes (grouped by plant types and plant parts) among different types of deposits [combustion features (white, reddish and black layers), bedding layers and light brown deposits], facies (as per Table 1) and units (2 WA.LR, 2 WA.UP, and 2

[1] An export permit for the analysis of sediment samples in Spain was issued by the South African Heritage Resources Agency (SAHRA) (permit number: 15987; permit holder: Irene Esteban).

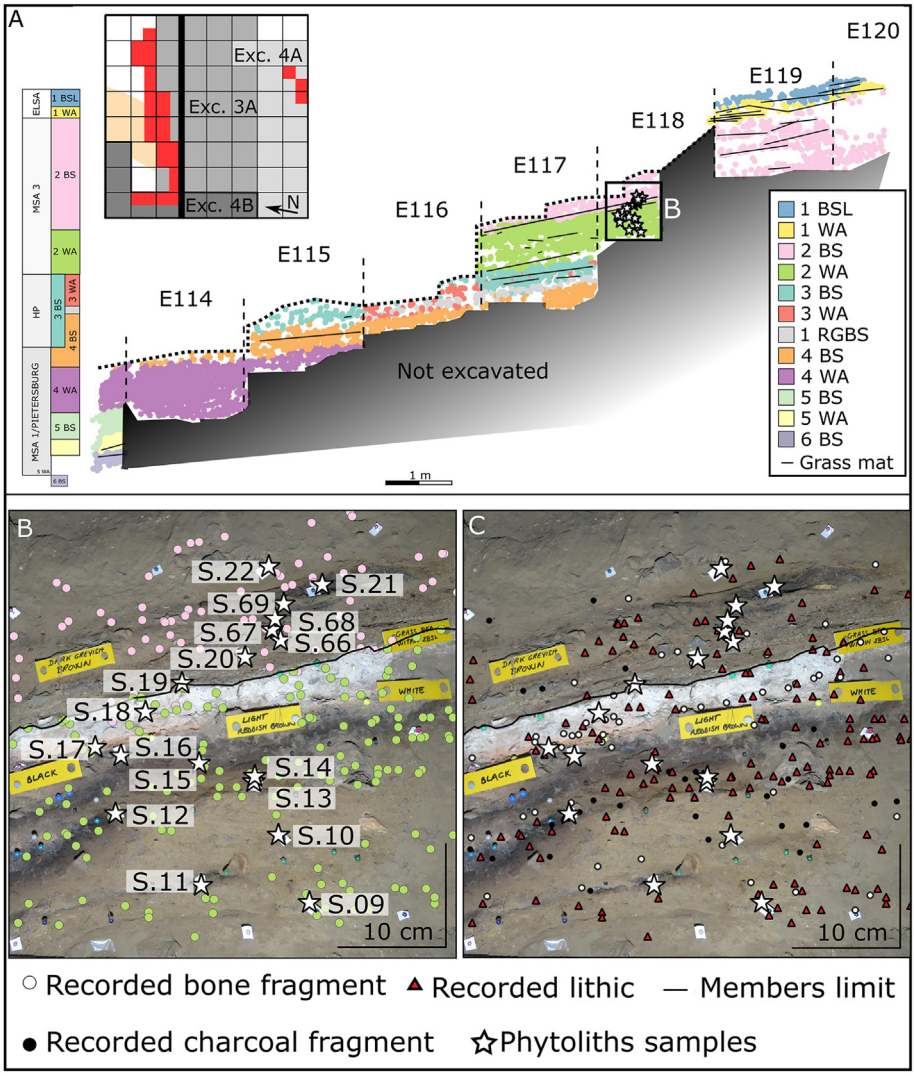

Fig. 2. Sample location. A. Stratigraphic sequence along the north wall of Beaumont's excavation 3 A rear trench showing excavations conducted from 2015 to 2019. The youngest deposits are towards the back of the cave on the right, and the oldest towards the centre of the cave on the left. The bold vertical line in the plan inset indicates the position of the section shown. The stars indicate where the samples were taken in square N109 E118 from Members 2 BS and 2 W A. **B.** Close-up of Member 2 BS.LR C (pink) and 2 W A (green) showing a field photograph with the location of samples (stars) and their numbers. **C.** Field photograph with point-plotted recorded bone fragments (white circles), recorded charcoal fragments (black circles) and lithic artefact distribution (red triangles) in unit 2 BS.LR C (in layers Orange silty, Dark Greyish Brown, Grass Mat 1 b, c, Grass Mat 2, Reddish Brown); unit 2 W A.UP (in layers White Ash, Black, Light Reddish Brown, Dark Greyish Brown, Grass Mat 1 b, c, Grass Mat 1 and 2, Grass Mat with bone); and unit 2 W A.LR (in layers Dark Brown Dijon, Dark Yellowish Brown Dino, Dark Yellowish Brown Dossy). The stars indicate the position of sediment samples taken from these layers for phytolith and FTIR analysis. (For interpretation of the references to colour in this figure legend, the reader is referred to the Web version of this article.)

BS.LR C) (SOM 1 - Tables S3 and S4). Samples from Facies III, VII, VI-III, and I-IV were excluded from the analyses for having only one representative sample. When significant differences were observed between certain groups, Dunn's pairwise comparison test with Bonferroni adjustments, a post-hoc, pairwise multiple comparison method, was also used to check for significant differences between groups. Nonetheless, the results obtained are tentative due to the small sample size. All statistical analyses used JMP®, Version 16. SAS Institute Inc., Cary, NC, 1989–2021.

Fourier Transform Infrared Spectroscopy (FTIR) was used to identify the bulk mineral components of the archaeological sediments to shed light on fire use and site occupation patterns, and better assess the state of preservation of the phytolith assemblages (Weiner, 2010). Sediment samples were lightly ground in an agate mortar and pestle under a hot lamp, mixed afterwards with ultra-pure potassium bromide (KBr) and pressed into pellets. Infrared spectra of the pellets were obtained at room temperature in the 4000–400 cm^{-1} region at 4 cm^{-1} resolution with a Nicolet iS5 spectrometer at the Laboratory of Archaeology of the University of Barcelona (Spain). Phase identification was performed using OMNIC 9 based on the FTIR reference collection of the Kimmel Centre for Archaeological Science of the Weizmann Institute of Science (http://www.weizmann.ac.il/kimmel-arch/infrared-spectra-library) and specialised literature (e.g. Chukanov and Vigasina, 2020; Weiner, 2010). The origin (geogenic, biogenic and pyrogenic) of the calcite (calcium carbonate) was assessed by applying the infrared grinding curve method developed by Regev et al. (2010), which is based on the measurement of the ratio of v_2/v_4 heights (874 cm^{-1} and 713 cm^{-1}, respectively) normalised to a v_3 height (1420 cm^{-1}). Shifts of silicate absorption bands in the 3800–3200 cm^{-1} and 1120–1000 cm^{-1} regions of a spectrum were tentatively used to assess differences in the exposure of sediments to heat (Berna et al., 2007). Because infrared spectra might show different heating signals depending on the clay types (Berna et al.,

2007) and we did not calibrate the effect of fire on local sediments or their clay size fractions, we will only make inferences with respect to the degree (higher versus lower) of heating. However, these interpretations should be regarded with caution until sediments from Border Cave are calibrated.

3. Results

Phytolith concentration in the Members 2 BS and 2 WA deposits in square N109 E118 ranged from 1.7 million to 14.8 million phytoliths (Table 1). We found statistically significant differences in phytolith concentration between members (x^2 = 9.5658, p = 0.0084) (SOM 1 − Table S3), and the pair-wise multiple comparison test (Dunn's) showed that 2 W A.LR C deposits have lower phytolith concentrations compared to 2 BS.LR (Z = −2.7756, p = 0.0055) and 2 WA.UP (Z = 2.2396, p = 0.0252) (SOM 1 − Table S4). In addition to phytoliths, diatoms (aquatic biogenic silica micro-remains) were also identified in every layer from both 2 BS and 2WA deposits, ranging from 0.5 to 17.4% of the total sum of silica particles counted (Table 1). Other siliceous micro-remains such as spicules of sponges and siliceous cysts of chrysophyte algae were also present, but rare. The modern soil outside the cave entrance and the site's surface samples yielded 3.5 and 0.8 million phytoliths, respectively (Table 1). Diatoms were identified at high frequencies in the modern soil outside the cave entrance, accounting for 32.6%, while they were absent in the site's surface sample (Table 1).

3.1. Phytolith taphonomy and mineralogy

The values of the four taphonomic indicators considered in this study are given in Table 1. The Spearman's correlation coefficient analysis used to assess the degree of preservation of the phytolith assemblage in both archaeological and control samples showed moderate and significant positive correlations between phytolith concentration and the % of articulated phytoliths (r = 0.5459, p = 0.0128) and between the number of morphotypes and the % of fragile morphotypes (r = 0.4797, p = 0.0323) (Table 2). Their distribution among types of deposits, members and facies, explored using the Kruskal-Wallis test, indicated that the % of articulated phytoliths yielded significant differences among types of deposits (x^2 = 12.2274, p = 0.0066) and facies (x^2 = 10.327, p = 0.0353), and the % of fragile morphotypes among types of deposits (x^2 = 7.9294, p = 0.0475) (SOM 1 − Table S3). The post-hoc test only yielded differences for the former, with control samples differing the most from bedding (Z = −2.66945; p = 0.0456) (SOM 1 − Table S4). The Spearman's correlation coefficient analysis conducted on 2 BS and 2 WA samples alone showed only a moderate but significant negative correlation between the number of morphotypes and the % of articulated phytoliths (r = −0.4927, p = 0.0378) (Table 2). The Kruskal Wallis and post-hoc tests found that only the articulated phytoliths showed significant percentage differences between types of deposits (x^2 = 8.7003; p = 0.0129) (SOM 1 − Table S3), with light brown deposits differing the most from bedding (Z = −2.4688; p = 0.0407) (SOM 1 − Table S4). Fig. 3 shows these results in a scatter plot with information on the sample number, type of deposit and facies. This illustrates that most light brown deposits have high numbers of morphotypes and a low % of articulated phytoliths. However, when looking at the facies classification we see contrasting results since not all facies show this correlation. This is, for example, the case with the Facies VI samples, where only samples 67 and 69 show a strong negative correlation between the number of morphotypes (high) and % of articulated phytoliths (low).

Figure S1 (SOM 1) illustrates some of the variability in FTIR spectra obtained from sediments attributed to the facies. Compound specificities for each layer are given in Table 1 and mentioned in the text when relevant. Sediment samples contain silicates (clay minerals, quartz and rhyolite), sulphates (gypsum), phosphates (carbonated hydroxyapatite), carbonates (calcite) and organic matter. Clay-rich archaeological deposits are normally composed of different clay minerals (e.g., montmorillonite, kaolinite, illite) that are sometimes difficult to differentiate based only on the infrared spectrum. The hydroxyl absorption bands around 3500 cm^{-1} are useful to differentiate clay minerals, but the sediments studied here do not show peaks at the appropriate absorption bands to be clearly discernible, probably due to the gypsum absorption bands in the O–H stretching region. At Border Cave, rhyolite and sandstone constitute the massive volcaniclastic breccia of which two facies (clast and matrix-supported) are exposed along the walls and roof of the cave (Backwell et al., 2018; Stratford et al., 2022). Gypsum was identified in all the samples from units 2 WA.UP and 2 BS.LR C in various concentrations (see Table 1). The layer Black (sample 16) from 2 WA.UP shows almost all the characteristic gypsum absorption bands (602, 669, doublet at 1114 and 1142, 1618, 3404 and 3549 cm^{-1}). Phosphate minerals in these deposits are mostly represented by carbonate hydroxyapatite. We observed in the spectrum of layer Black (sample 16) that the peak at 603 cm^{-1} is slightly higher than the peak at 567 cm^{-1}, which is typical of carbonate fluorapatite and could account for its presence (Geiger and Weiner, 1993). Finally, the broad shape of the curves of some spectra (samples 10, 13, 15, 19 or 69 – see Figure S1 in SOM 1) around the 600-400 cm^{-1} region could be explained by the presence of iron oxides, such as hematite, together with carbonate hydroxyapatite and silicates. However, the unclear identification of hematite characteristic peaks or shoulders prevents us from identifying this mineral phase in our samples with certainty.

3.2. Plant phytolith morphological distribution

The modern surface sample from the vegetated area outside the cave is dominated by the presence of Grass Silica Short Cell phytoliths (GSSCPs; 66.1%) and ELONGATES ENTIRE (14.7%), while eudicotyledonous leaves (hereafter referred to as eudicots) and SPHEROIDS were identified in low frequencies (0.8 and 1.2%, respectively) (Table S2 in SOM 2 and Fig. 4). The sample from the site's surface is also dominated by the presence of GSSCPs (42.5%) and ELONGATES ENTIRE (12.5%) together with SPHEROIDS (13.8%) (Fig. 4).

Most of the 2 BS and 2 WA samples present a phytolith assemblage characterised by the abundant representation of phytoliths from grasses (i.e. GSSCPs) (Fig. 5a) and other graminoids (i.e. ELONGATES with decorated margins) (Fig. 5b), while there are lower frequencies of phytoliths associated with a variety of other monocot plants [(i.e. ELONGATES ENTIRE, BULLIFORMS) (Fig. 5c) and all hair types (ACUTE BULBOUS) including trichomes, prickles, and cystoliths)]. Characteristic phytoliths of eudicot leaves and BLOCKY and SPHEROID morphologies were recorded even in fewer frequencies (Figs. 4 and 5d). We observed in various samples a robust BLOCKY morphotype that has a blocky polyhedral basal part and an upper conical part that are connected through a concavity with a striate surface (Fig. 5e and f). This morphotype doesn't resemble any BLOCKY type observed before in South African plants (Esteban, 2016; Esteban et al., 2017b; Murungi, 2017; Esteban and Murungi, from personal experience). Although they do resemble those produced by *Commelina* seeds (Eichhorn et al., 2010), they are larger in size (height mean, 48 μm; width mean, 58 μm) but with similar height/width ratios of 0.6–1.1. They also have a certain resemblance to Marantaceae seed phytoliths (Piperno, 2006), but this family is not native to South Africa. Therefore, we refer to them in this study as BLOCKY cf. *Commelina* for

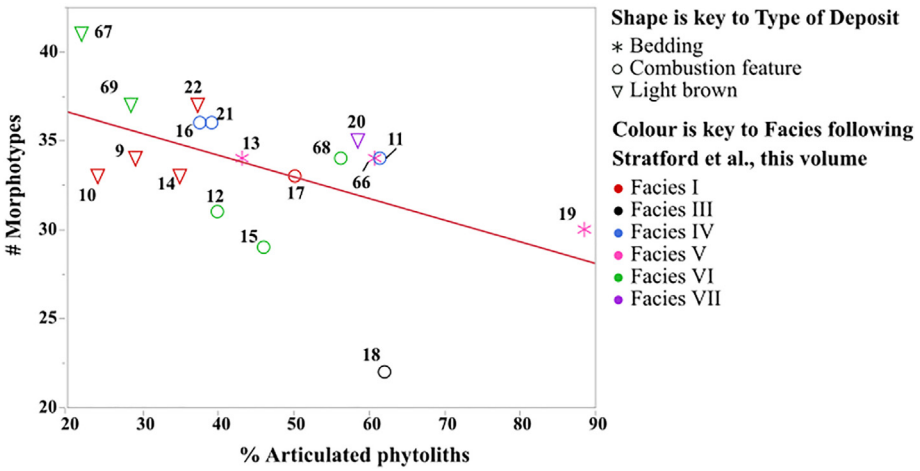

Fig. 3. Phytolith fragmentation. Graph showing the relationship between the number of morphotypes and the percentage of articulated phytoliths among different types of deposit (bedding layers, combustion features and light brown sediments) and facies (following Stratford et al., 2022). The red line indicates the line of best fit. Spearman's correlation coefficient and *p*-value of the whole dataset is $r = -0.4927$, $p = 0.0378$ (Table 2). Facies I, Massive sands; Facies III, Ash; Facies IV, Massive charcoal; Facies V, Laminated organic matter; Facies VI, Homogeneous anthropogenic components; Facies VII, Homogeneous (with stratified) anthropogenic components. (For interpretation of the references to colour in this figure legend, the reader is referred to the Web version of this article.)

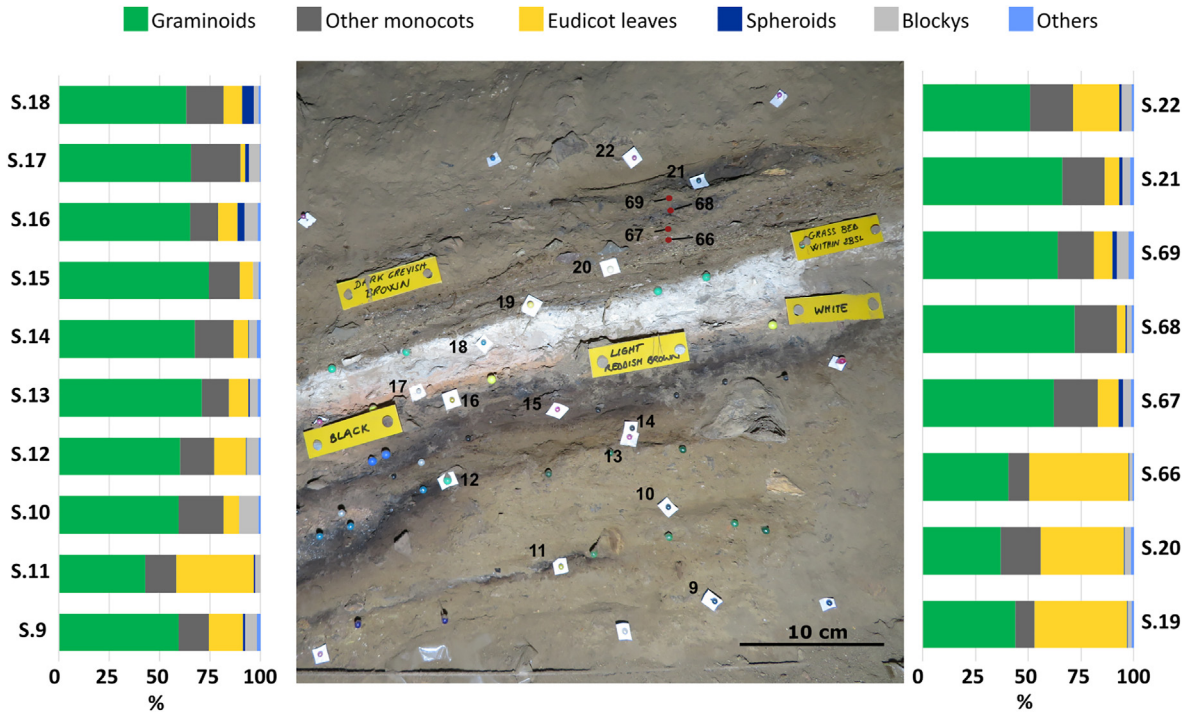

Fig. 4. Phytolith morphological distribution. Field photograph showing the sample location and histograms of stacked bars showing the plant phytolith distribution for each sample. The Y-axis indicates the sample number.

simplification (Table S2 in SOM 2). If future comparative studies from modern plants from the region confirm that these Blocky morphotypes are produced by *Commelina* seeds, this finding could represent the identification of Commelinaceae seed phytoliths for the first time in the South African phytolith record. The study of Commelinaceae plants for their phytolith content will be the next step in future phytolith studies at the site. Finally, eudicot leaf epidermal phytoliths are well represented but in variable concentrations, being the dominant plant type in some samples (e.g. S.66, 46.1%; S.19, 42.4%) while rare in others (e.g. S.17, 0.7%) (Fig. 5g).

Statistically significant differences were found between types of deposits and Elongates with decorated margins ($x^2 = 7.5056$, $p = 0.0235$), elongates entire ($x^2 = 7.2556$, $p = 0.0266$) and eudicot leaf phytoliths ($x^2 = 6.0537$, $p = 0.0485$) (SOM 1 – Table S3; Fig. 6a). The pair-wise multiple comparison test (Dunn's) showed that bedding layers differed the most from light brown deposits ($Z = 2.5335$. $p = 0.0339$) by having the lowest number of elongates entire (SOM 1 – Table S4). Elongates with decorated margins, representing graminoids, have their highest frequencies in combustion feature layers, and these differed the most from light brown deposits ($Z = -2.6854$, $p = 0.0217$) (SOM 1 – Table S4). No significant differences were detected in the multiple comparisons analysis for

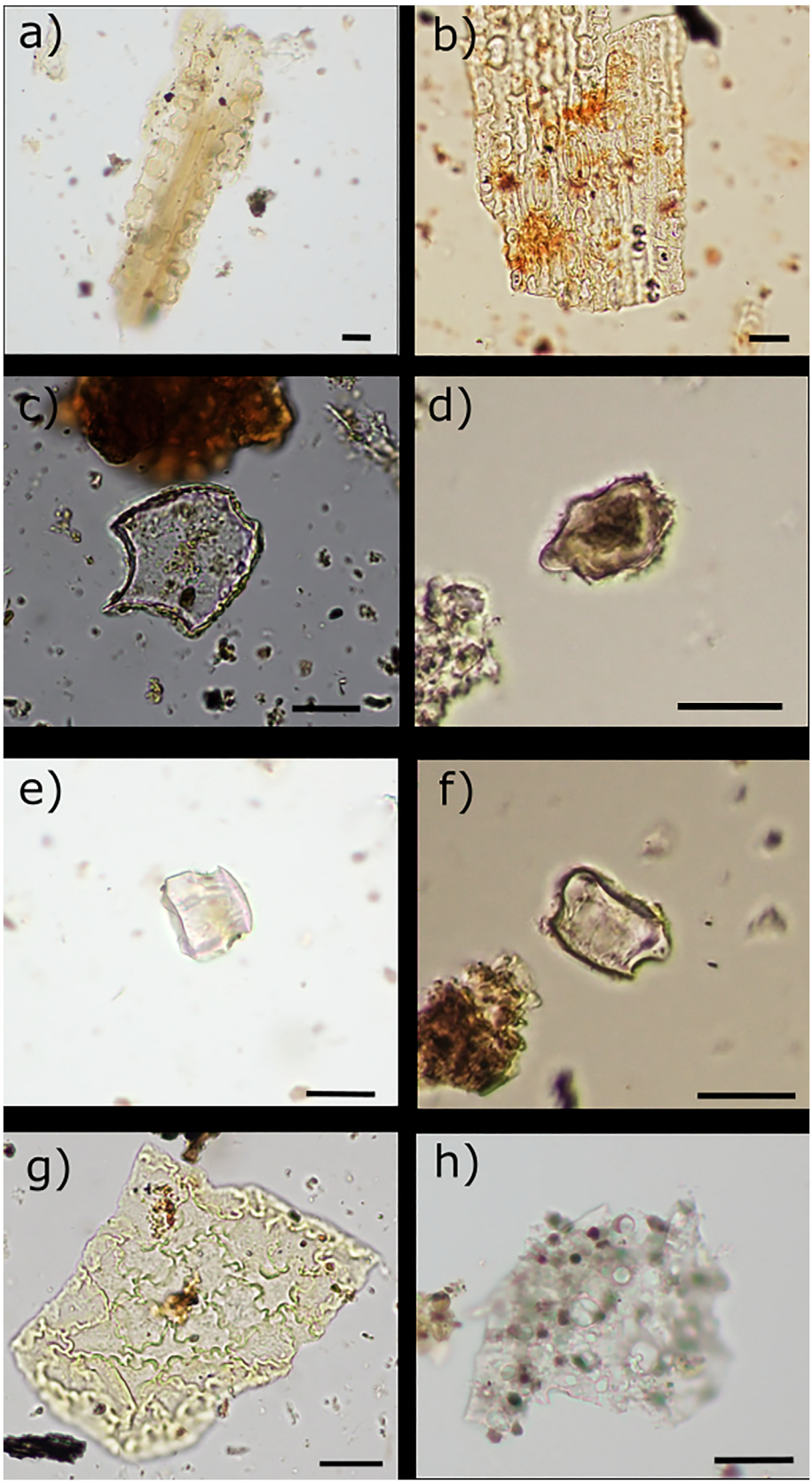

Fig. 5. Representative phytolith photographs. Micro-photographs of phytoliths identified in the Border Cave Member 2 BS and 2 W A deposits; a) silicified grass epidermis showing articulated epidermal elongates and short cell bilobates (S. 19); b) silicified grass epidermis showing articulated epidermal elongates with decorated margins, short cell bilobates and stomata (S. 17); c) Bulliform cell (S. 22); d) Spheroid decorated (S.18); e-f) Blocky cf. *Commelina* (S.19 and 10); g) Articulated eudicot leaf epidermal sinuate (S. 66); h) Weathered phytolith (S.18). Scale bars represent 20 μm.

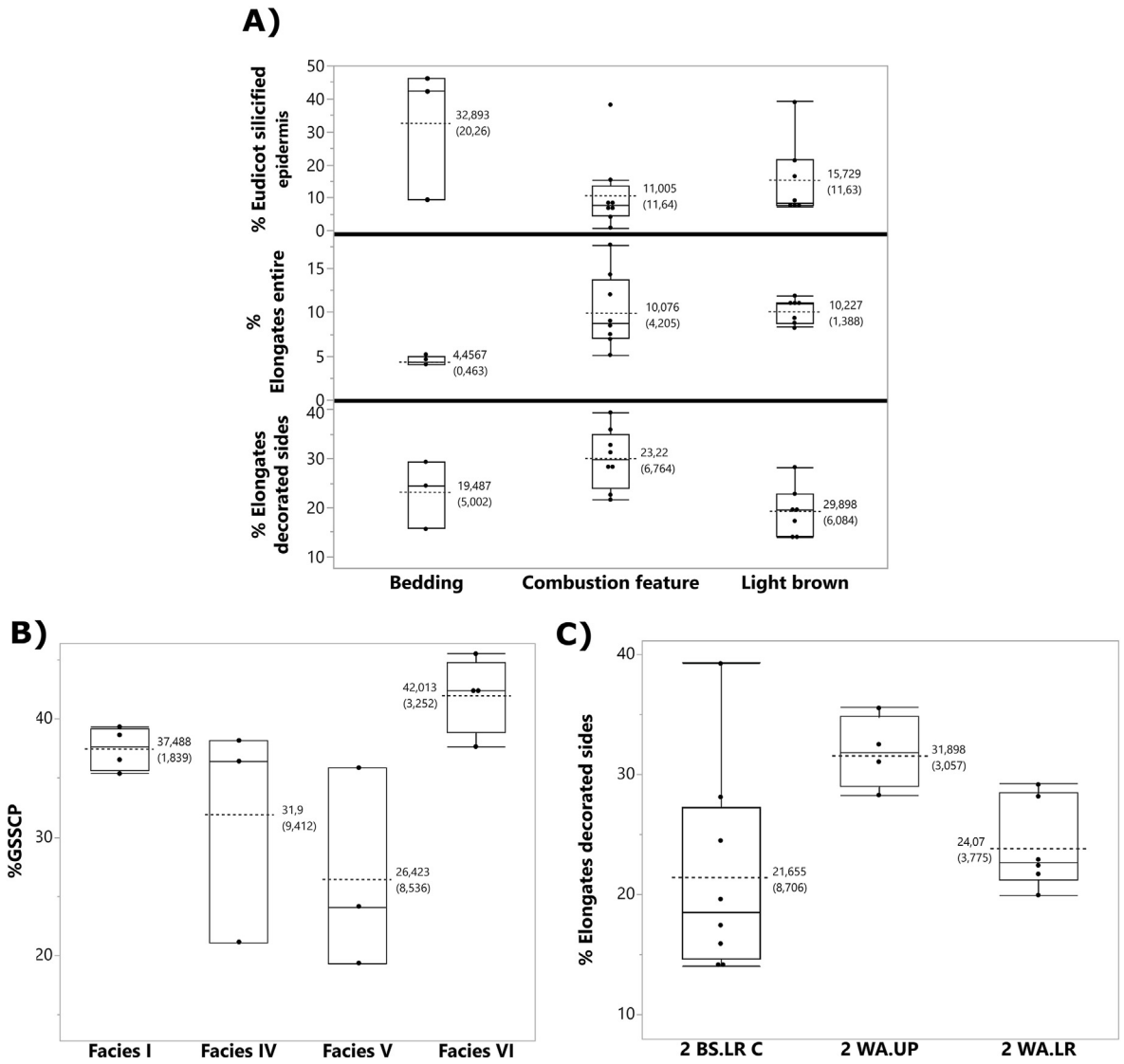

Fig. 6. Graphical representation of statistical analysis. Box plots documenting significant differences in the percentage of phytoliths found in A) different types of sediments, B) facies, and C) member unitss. Facies I = Massive sands; Facies IV = Massive charcoal; Facies V = Laminated organic matter; Facies VI = Homogeneous anthropogenic components. Box-plot description: the mid-line indicates the median, boxes indicate the standard error ±, the standard deviation is indicated by the whiskers, and outliers extended beyond the whiskers. Means and standard deviations are given next to each's groups mean lines (dashes).

eudicot leaf phytoliths. GSSCPs yielded statistically significant differences between facies ($x^2 = 8.2333$, $p = 0.0414$) (SOM 1 – Table S3; Fig. 6b). Although no differences were observed in the multiple comparisons analysis, all samples from Facies I and VI had frequencies of GSSCPs higher than the grand mean as opposed to those from Facies IV and V. Finally, ELONGATES with decorated margins were the only phytolith group that yielded statistically significant differences between member units ($x^2 = 6.769$, $p = 0.0339$), and 2 WA.UP had the highest frequencies, differing the most from 2 WA.LR ($Z = 2.5427$, $p = 0.033$) (SOM 1 – Table S3; Fig. 6c).

A description of the phytolith and mineralogical composition of sediment samples from different layers in units 2 BS.LR C, 2 WA.UP and 2 WA.LR in square N109 E118 is presented from bottom (oldest deposits) to top (youngest deposits) (Table S2 in SOM 2; Fig. 4).

The bottom of the profile sampled for this study was from 2 WA.LR, which is characterised by a relatively thick light brown sedimentary unit that includes layers Dark Yellowish Brown Dossy and Dark Yellowish Brown Dino (samples 9 and 10, respectively). These two layers are truncated in this part of the sequence by a thin black lens (sample 11 from Dark Yellowish Brown Dossy). Phytolith concentration ranges in this part of the sequence from 4.6 million to 6.6 million phytoliths. The % of weathered morphotypes is less than 5% and diatoms range from 3.76% to 6.41% (Table 1). The thin black lens (sample 11 Dark Yellowish Brown Dossy) differs from the light brown deposits (samples 9 Dark Yellowish Brown Dossy and 10 Dark Yellowish Brown Dino) by having higher frequencies of characteristic articulated eudicot epidermal leaf polyhedral and sinuate phytoliths (Fig. 4; Table S2 in SOM 2). The mineralogical composition is characterised by the presence of silicates (quartz and rhyolite) and clay minerals. Organic matter is present in the light brown sediment and not in the thin black layer (Table 1).

Above these, a layer called Dark Brown Dijon (sample 13) consists of a thin sediment stratum in which some plant material is still preserved. It yielded 5.5 million phytoliths and contained the highest frequency of characteristic sedge phytoliths (5.6%). The southern part of what seems to be the same layer Dark Brown Dijon (sample 12) is darker in colour, and plant material appears not to be preserved. Here, phytoliths were identified in lower numbers (1.7

million). Although the mineralogical composition of Dark Brown Dijon samples (12 and 13) is the same, the major Si–O–Si stretching peak of the dark lens (sample 12) is situated at 1038 cm^{-1} while that of the bedding layer Dark Brown Dijon (sample 13) is situated at 1034 cm^{-1}.

Overlying these deposits, at the contact between the Lower and Upper sections of unit 2 WA, there is a thin layer of light brown sediment (sample 14, layer 'contact between Dark Brown Dijon and Dark Yellowish Brown Devo') similar in colour and texture to the unit below it (Dark Yellowish Brown Dossy and Dark Yellowish Brown Dino, samples 9 and 10 respectively; see Table 1 and Fig. 4). This light brown contact layer (sample 14) presents a slightly higher phytolith concentration (6.1 million) than the bedding layer Dark Brown Dijon (sample 13) and a high % of diatoms (10.5%). Here, at the contact (sample 14), grass phytoliths and elongate morphologies representing both graminoids and other monocots dominate the phytolith assemblage, with eudicot leaf and other phytolith types being less represented. These deposits have the same mineralogical composition as the other light brown sediments from Dark Yellowish Brown Dossy and Dark Yellowish Brown Dino (samples 9 and 10).

Unit 2 WA Upper (2 W A.UP) consists of a succession of dark brown (sample 15, layer Light Reddish Brown) and black (sample 16, layer Black) sediments, which are overlain by a thick reddish layer (sample 17, layer Light Reddish Brown). These are all directly overlain by a thick white ashy layer (sample 18, layer White Ash) that marks the last of the Member 2 WA deposits (see Table 1 and Fig. 3). The sediment samples from the dark brown (sample 15) and light black (sample 16) deposits present a similar phytolith concentration (7.6 and 6.3 million phytoliths, respectively). Diatoms are also well-represented, comprising between 7.6 and 8% of the silica particles counted. Although the phytolith assemblages present in the two samples do not differ substantially, we find that the base of these dark deposits (sample 15) has a slightly higher presence of graminoids (both grass and sedge phytoliths, and other graminoid phytolith morphotypes). Conversely, the upper part of these deposits (sample 16) is bare of characteristic sedge morphotypes, has higher frequencies of eudicot leaf phytoliths and blocky morphologies, and it contains spheroids, which are absent in sample 15. The mineralogical composition of these two samples is also different, with the dark brown sediment layer (sample 15) mainly composed of silicates (quartz, rhyolite and clay minerals) and traces of calcite, while gypsum, clay minerals and carbonate hydroxyapatite dominate in the black layer (sample 16). The Light Reddish Brown layer (sample 17), which is stratigraphically above layer Black (sample 16) and below layer White Ash (sample 18), reached 14.4 million phytoliths and showed the highest presence of diatoms (17.4%). The phytolith assemblage from this sample stands out for having the highest presence of ENTIRE (17.6%) and decorated margins (33%) of ELONGATES, and the lowest occurrence of eudicot leaves (0.7%). The main mineral component of this layer is gypsum and carbonate hydroxyapatite, in addition to clay minerals and quartz. The White Ash layer (sample 18) has the highest phytolith concentration of all the samples (14.7 million) but most of the identified phytoliths were weathered (76.1%) (Fig. 5 h). Of the phytoliths that had a consistent morphology, we observed a high frequency of spheroids (5.7%), the highest among all the samples. From a mineralogical perspective, this layer presents high quantities of calcite from wood ash [(normalised v_2 peak height = 354; normalised v_4 peak height = 108; FWHM – full width at half maximal height value of the v_3 peak = 115) (Regev et al., 2010)], as well as other minerals such as clay minerals, quartz, gypsum and carbonate hydroxyapatite. The major Si–O–Si stretching peak of the ash is located at 1034 cm^{-1}. This differs from the deposits below, which show the major Si–O–Si stretching peaks at 1042 cm^{-1} (Light Reddish Brown) and 1038 cm^{-1} (Black layers, samples 16 and 15).

Lying directly on top of the White Ash layer are three bedding layers. Grass Mat with bone (sample 19) and Grass Mat 1 b, c (sample 66), which are both classified as Facies V and at the time of phytolith sampling preserved plant material. These layers are separated by a light brown layer of what appears to be a mixed debris deposit (Grass Mat 1 and 2, sample 20), which was classified as Facies VII and did not preserve plant material at first sight. These deposits have a phytolith concentration ranging from 10.1 to 14.8 million phytoliths and a low % of weathered morphologies (Table 1). Only sample 66 has a slightly higher presence of diatoms (7.1%) in comparison with that observed from the bedding layer below (sample 19). The phytolith assemblage of these three layers (samples 19, 20, 66) is quite homogeneous, dominated by the presence of eudicot leaf epidermal phytoliths with polyhedral and sinuate shapes, which make up between 39% and 46% of the total. Grass Mat 1 b, c (sample 66) has very distinctive eudicot leaf articulated jigsaw phytoliths, which only occur in this sample (Fig. 5g; Table S2 in SOM 2). From a plant phytolith distribution point of view, the only sample homologous to this one is that of layer Dark Yellowish Brown Dossy (sample 11), a thin black lens in 2 WA.LR. Mineralogically, we note that the layers still preserving plant material, such as Grass Mat with bone and Grass Mat 1 b, c (samples 19 and 66), have a similar mineral composition, with high virtual quantities of gypsum, as well as clay minerals, carbonate hydroxyapatite, and organic matter. We noted that the light brown layer (sample 20) has little gypsum.

The upper part of the sequence consists of a succession of light brown and black layers that do not have plant material preserved (samples 67, 68, 69, 21 and 22). These deposits show similar phytolith concentrations, ranging from 10.1 to 13.7 million phytoliths, except for the light brown layer Dark Greyish Brown (sample 69) which yielded fewer phytoliths (5.5 million phytoliths). Diatoms are present in all these samples, ranging from 3.6% to 8.1%. The phytolith assemblage in these samples does not differ much from that of the other samples in 2 BS.LR C or analysed in this study, nor between them. Only samples 68 (Grass Mat 1 b, c) and 22 (Dark Greyish Brown to Orange Silty) have slightly different plant composition assemblages, where ELONGATES with decorated margins show the highest frequencies in sample 69 (29.3%), and sample 22 has the highest eudicot epidermal leaf phytolith frequencies among all the 2 BS.LR C samples analysed in this study (21.5%). Their mineralogical composition is quite homogeneous, with clay minerals being the main mineral component, followed by various concentrations of gypsum and carbonate hydroxyapatite, and organic matter in lesser amounts. The major Si–O–Si stretching peaks are located at 1042 cm^{-1} for sample 68 and 1038 cm^{-1} for samples 67, 69, 21 and 22.

4. Discussion

4.1. Taphonomic considerations

The mineralogical composition of archaeological deposits provides useful information on the source material of the sediments, depositional environments, weathering, and post-depositional processes (Weiner, 2010). FTIR analysis of 2 BS and 2 WA deposits in square N109 E118 shows variability in the mineralogical composition of different layers that are not associated with the type of deposit or facies (Table 1 and SOM 1 – Figure S1). This is also the case for the phytolith morphological distribution (Fig. 4; Table S2 in SOM 2). We interpret this evidence as being the result of nuanced primary or secondary processes taking place at the site that were not recognised at a microscopic scale. Intra-facies mineralogical

variability can be attributed to minor differences in primary sediment composition and post-depositional processes that can, over time, generate sediments with similar macroscopic attributes (see Stratford et al., 2022 for discussion). Significant variability may manifest locally, both vertically and laterally, as evident from lateral structural, textural, and compositional changes.

The presence of highly unstable minerals such as carbonate hydroxyapatite and gypsum, mainly in 2 BS.LR C and minimally in 2 WA.UP, indicates a good state of preservation and integrity of these deposits. The presence of carbonate hydroxyapatite in archaeological sites can derive from guano, the stabilization of organic matter once degraded, and bone (Lippmann, 1973; Karkanas and Goldberg, 2010; Weiner, 2010). All three scenarios might have taken place at Border Cave. They are difficult to differentiate from each other because: (i) bats live in the cave today and probably did so in the past; (ii) organic matter from food and plant waste might have been abundant at the site. However, the organic matter observed in our FTIR analysis and that of Stratford et al. (2022) probably derives from charcoal and the decay of desiccated plant material (see SOM 1 – Figure S1, Facies V, S.66 plant material) rather than from old food and plant waste; and (iii) bone fragments occur in practically all layers throughout the sedimentary sequence. Its presence in these units also occurs in the more anthropogenic layers of the 2 BS and 2 WA deposits studied here. Conversely, carbonate hydroxyapatite is absent in 2 WA.LR deposits, a unit mostly comprised of geogenic components with a low frequency of cultural material and anthropogenic structures. Fluorite can be leached from some rhyolitic host rocks as an authigenic mineral (Scaillet and Macdonald, 2004) and the presence of carbonate fluorapatite in layer Black (sample 16) of 2 WA.UP could be derived from localised *in situ* decay of some rhyolitic clasts. Alternatively, fluorite could derive from the exposure of bone to fluoride, derived from moisture leaching fluorite from the cave walls and percolating through the sediments. If the latter was the case, then bone should be well-preserved in that unit (e.g. Toffolo et al., 2015). Bone is indeed well represented in this member unit, but its surface preservation is poor and, as discussed by Stratford et al. (2022) and Backwell et al. (2022), this is probably due to surface modification by ancient and modern invertebrates inhabiting the deposit, and the effects of burning. Further mineralogical analysis of sediments and bone, and controlled bone modification experiments with a suite of invertebrates currently inhabiting the deposit need to be undertaken to better comprehend bone taphonomy at the site. The most common carbonate in archaeological sites is calcite (calcium carbonate), which can derive from the burning of wood (pyrogenic calcite), the presence of shells (biogenic calcite), or related to saturated solutions of water percolating from the cave walls and the roof (geogenic calcite) (Karkanas and Goldberg, 2010; Weiner, 2010). At Border Cave, although minor contributions of calcites could derive from interbedded sandstones within the rhyolite, it may be mainly pyrogenic or biogenic because the site is not hosted within a highly calcareous bedrock (Backwell et al., 2018). We further discuss, in the section devoted to pyrotechnology, the origin of the calcium carbonate identified as the main compound in one of our studied samples. Gypsum, a common sulphate mineral found in caves, forms due to the evaporation of water from mineral-rich sediments, which in Member 2 WA could be related to a dry phase following the low energy water runoff that formed channels and mudflow (Stratford et al., 2022) or localised, spotty precipitation on exposed surfaces during drying after interaction with mists that enter the cave (Beaumont, 1978; Backwell et al., 2018). At Border cave, gypsum nodules are characteristic of secondary gypsum (Backwell et al., 2018), especially considering its association with carbonate hydroxyapatite (Table 1; Shahack-Gross et al., 2004), formed through the breakdown of organic matter or guano (Shahack-Gross et al., 2004; Schiegl and Conard, 2006).

Phytoliths were identified in every studied layer from the 2 BS and 2 WA deposits in square N109 E118. The origin of phytoliths recovered in archaeological deposits is often considered a matter of controversy. They can be introduced by human agency or natural phenomena such as plants growing at the site, by wind or water runoff, or by nesting or occupying animals. At Border Cave, most layers yield lithic cultural material and anthropogenic structures (i.e. bedding and combustion features) that support the contention that substantial components of the deposits are anthropogenic in origin. The fact that some bedding may have been woven (Sievers et al., 2022) shows that past site occupants intentionally introduced and manipulated grasses at least 40,000 years ago in Africa. The differences observed between the control samples and 2 BS and 2 WA samples (i.e. a generally lower phytolith concentration, lower representation of eudicot leaf phytoliths, and lower % of articulated phytoliths and fragile morphotypes) evidence the different histories (natural versus anthropogenic) of the phytolith assemblages. Furthermore, plants are unlikely to grow inside Border Cave because sunlight only reaches midway into the shelter in the summer months and only in the late afternoon for a short time, and the area sampled is towards the back of the shelter. In addition to insufficient sunlight to support plant growth, regular, abundant water entering the shelter is unlikely. Despite some evidence of channels, mudflows, and reworking of ash lenses at numerous levels of the sequence (Stratford et al., 2022), the mechanisms of water introduction are not yet clear. If vegetation grew at the entrance of the cave ~60 ka ago, it is plausible that some plant material or plant phytoliths were incorporated into the sediments by natural means. Consequently, the phytoliths studied here must have mostly derived from plants introduced by humans and only to a lesser extent non-human agents such as wind or nesting and burrowing animals.

One of our goals was to decipher the taphonomic histories of plant phytoliths from the complex succession of distinct vertically overlapping combustion features, bedding layers and light brown sediments. The area sampled here is towards the back of the shelter, so disturbance by trampling and domestic activities would have been constant, but variable depending upon when people visited the site, the number of people in the group, the length of their stay and where, within the large cave space, different activities were practised. In this sense, special attention has been given to the predominantly geogenic light brown layers, which contain few anthropogenic artefacts. Overall, the taphonomic analysis indicates that the phytolith assemblage is well-preserved and that little weathering took place in units 2 WA.UP and 2 BS.LR C (Table 2 and Fig. 3). The chemical stability and integrity of the phytolith assemblages in these units imply that human occupations at the site might have been intense (high phytolith concentration), but perhaps did not last long and were intermittent (low rates of phytolith breakage). This is well supported by the geoarchaeological, faunal and stratigraphic evidence (Stratford et al., 2022). Nonetheless, high rates of phytolith breakage might have taken place in the light brown layers of 2 WA.LR and 2 BS.LR C (Fig. 3), which correspond to Facies I (samples 9, 10, 14 and 22) and VI (samples 67 and 69) of Stratford et al. (2022) (see Table 1). Facies I are mostly geogenic deposits with little cultural material (Fig. 2) and lack anthropogenic structures such as bedding or combustion features (Stratford et al., 2022). We observed that Facies I deposits from 2 WA.LR (samples 9, 10 and 14) are the only samples whose FTIR spectra show rhyolite but also do not preserve unstable minerals such as carbonate hydroxyapatite (Table 1). The identification of rhyolite in these spectra can be explained by the higher frequency of roof spall from the rhyolite host rock. These results are consistent with the Stratford and colleagues' (2022) facies

interpretation and support the interpretation that these sediments are formed primarily by the accumulation of geogenic authigenic minerals and represent long periods of slow sediment accumulation during which humans might have visited the site sporadically. Slow rates of sediment accumulation would have resulted in the site's surface sediments being exposed for extended periods of time allowing cumulative turbative processes, homogenising the deposits, and facilitating the breakage of phytoliths and the diagenesis of unstable minerals. A different story is observed from the light brown deposits of 2 BS.LR C (samples 69, 67 and 20), which were classified as Facies VI (homogeneous anthropogenic components) by Stratford et al. (2022). They classify this facies as massive silty sand-supported facies with minor inclusions of ash and other anthropogenic components such as desiccated plant remains, wood and charcoal, knapping debris, ochre grains, and both burnt and unburnt microfauna and macrofauna bones. Facies VI light brown deposits differed in their phytolith and mineralogical records from Facies I light brown deposits of 2 WA.LR (samples 9, 10 and 14) by showing a higher phytolith concentration (stronger anthropogenic input in the form of human introduction of plants), the presence of carbonate hydroxyapatite (the mineral trace of a past concentration of organic matter, bone or diagenetically altered ash) and yet high rates of phytolith breakage (higher trampling). These differences indicate a different formation history, with humans contributing more significantly to the creation of Facies VI sediments. Our results thus further support the classification of Facies VI light brown deposits as a mixture of geogenic authigenic (dominance of quartz and clay minerals) and anthropogenic detritus (high phytolith concentration) which suffered various post-depositional processes caused partially by past site occupants through trampling (high % of phytolith breakage). Nonetheless, other Facies VI layers in this study (samples 12, 15 and 68) do not fit this tendency and show low rates of phytolith breakage (i.e. high % of articulated phytoliths, Fig. 3). These results indicate different moments of occupation or perhaps that different areas of the site were affected differently.

4.2. Plant uses at Border Cave

The morphology of phytoliths from 2 BS to 2 WA indicates plant cells that belong to a variety of plants (grasses, sedges, herbs, shrubs and/or trees) and different plant parts (inflorescences, culms, leaves and wood) that would have been commonly used by site occupants for a variety of purposes (Table S2 in SOM 2). Phytoliths that occur in many graminoids and monocots were identified in high numbers throughout the sequence studied here, irrespective of the type of deposit, stratigraphic provenance, or facies. However, many of the identified phytoliths in our deposits occur in the epidermis of the leaves and culms of graminoids, as well as in other monocot plants. Of the grass phytoliths identified, Panicoideae and other PACMAD grasses dominated, and Chloridoideae were also well represented, which are all C_4 grasses. Although C_3 Pooideae grasses (GSSC CRENATE) were also recorded these were identified in low frequencies. It is plausible that other grass subfamilies were collected but were unrecognised. The high representation of graminoids and monocots at Border Cave might be mostly due to their use by past inhabitants for a variety of reasons such as bedding construction (Backwell et al., 2018; Wadley et al., 2020a; Sievers et al., 2022). However, based on the practices of modern peoples of South Africa (van Wyk and Gericke, 2000; Gebashe et al., 2019; Nortje and van Wyk, 2019), grasses and other graminoids could have been used at Border Cave for other reasons also, such as for crafts (basketry), construction (e.g. windbreaks) or medicinal purposes.

4.2.1. Pyrotechnology and use of plants as fuel

The 2 WA.UP stratified combustion feature in square N109 E118 consists of, from top to bottom, a white ashy layer (White Ash), a reddish layer (Light Reddish Brown), and a thick black layer (Black). Layer White Ash is mainly composed of wood-ash calcite (Regev et al., 2010) indicating that wood, probably dry (Albert and Cabanes, 2007), was the main source of fuel. Weathered phytoliths constituted 76.1% of the phytoliths counted, which indicates that the phytolith assemblage was negatively affected by burning or the pH of the ashes (Cabanes et al., 2011). Although graminoids, including grasses and sedges, constitute 65.5% of the phytolith assemblage, this layer yielded the highest frequencies of spheroids among all the samples, and this is evidence of the use of wood as the primary fuel (Fig. 4). As previously reported at other archaeological sites, the presence of non-woody phytoliths in ash layers, such as grass phytoliths, can be partially related to contamination as they could have been introduced together with the wood used as fuel, since the contribution of grass phytoliths in South African wood phytolith assemblages may constitute up to 44% (Esteban et al., 2017a). It is plausible that dry grass was also used as tinder and kindling, or that old or damaged grass crafts or bedding were intentionally burned to dispose of them. We cannot rule out that some phytoliths were also blown into the hearths from surrounding sediments of bedding structures. However, we discard that some of the non-wood phytoliths come from mixing with the sediments that constitute the base of the hearth because no mixing of minerals (mainly that of calcite) is observed (Table 1).

Recent fire experiments conducted by some of us (Esteban and Sievers), the results of which are yet to be published, showed the same succession of layers. In four experimental fires, we observed that the ashy layer was the only layer of the combustion feature associated with the intentional burning of plant material. We can say from our observations that the reddish and black layers represent the substrate where the fires were built. This observation is supported by previous experiments conducted by Mallol et al. (2013). The difference in colour (reddish versus black) might relate to their distance from the fire and the temperatures of the soil underneath (Goldberg et al., 2009; Miller et al., 2010; Mallol et al., 2013), with the reddish layer being closer to the fuel and the sediments suffering more severe alteration. The strong reddish colour of the Light Reddish Brown layer (sample 17), and the location of the major Si—O—Si stretching peak at 1042 cm^{-1} indicates that this layer might have been exposed to higher temperatures than the Black layer underneath (sample 16), whose spectra show the major Si—O—Si stretching peak at 1038 cm^{-1}. Likewise, the traces of calcite (shoulder at 875 cm^{-1}, see SOM 1 — Figure S1, Facies I, S.17) in the Light Reddish Brown layer suggests that there may have been little or no mixing between the ash and the sediment below, indicating that the ashy layer studied here is not the result of ash dumping or rake-out. These results further support the facies interpretation of this hearth (combustion feature 7) in Stratford et al. (2022). On the other hand, layers Light Reddish Brown and Black layers of 2 WA.UP might represent the partial burning of plant material that was present in the soil underneath the hearth prior to its construction. The effect of fire might have affected layer Black by charring the plant matter, changing the sediment colour and perhaps also the mineralogy. Complete combustion and reddening of soils did not happen because they were further away from the coals. Therefore, the facies association of layer Black (Facies IV in Stratford et al., 2022) should be associated with human activities that preceded this fire. This is something to consider when studying this facies in future.

4.2.2. The <60,000-year-old bedding layers

Past hunter-gatherers, both modern humans and Neanderthals,

have deposited bundles of plant material on cave floors to create areas to sleep and work on (Cabanes et al., 2010; Wadley et al., 2011; Weinstein-Evron et al., 2012; Ramsey et al., 2018). Border Cave preserves the world's oldest record of such structures (Wadley et al., 2020a) that occasionally still preserve desiccated plant material (Backwell et al., 2018). In southern Africa, grasses appear to have been the main plants used for the construction of bedding at Border Cave (Sievers et al., 2022; Wadley et al., 2020a) and other graminoids were reported to have been used for bedding construction, such as sedges at Sibudu (Wadley et al., 2011) and perhaps restios, a graminoid family considered diagnostic of the Fynbos biome, at Pinnacle Point 5–6 (Esteban et al., 2018).

Three layers sampled for this study preserved desiccated plant material, and these are Dark Brown Dijon in 2 WA.LR (sample 13), Grass Mat with bone in 2 BS.LR C (sample 19), and Grass Mat 1 b, c in 2 BS.LR C (sample 66). Although these bedding layers showed a similar plant phytolith composition to that observed in other types of deposits, they differed in terms of their abundance, and this is mostly observed in the distribution of eudicot leaf phytoliths. For example, of these three bedding layers, only layers Grass Mat with bone and Grass Mat 1 b, c from 2 BS.LR C (samples 19 and 66) showed high frequencies of eudicot leaf phytoliths (42.38% and 46.15%, respectively). Sievers et al. (2022) also found eudicot leaves in bedding deposits, particularly in 2 W A, and two species were identified: *Sideroxylon inerme* (White Milkwood, Sapotaceae family) and *Chionanthus foveolatus* (Pock Ironwood, Oleaceae family). Eudicot epidermal tissue silicification is not extremely high and varies among families (Piperno, 2006). For example, phytolith production of southern African eudicot leaves is relatively low (Esteban et al., 2017a), and their phytoliths are not commonly found in modern soils of extant habitats even when trees dominate the environments (Esteban et al., 2017a, Esteban et al., 2017b). This is also observed in the soil outside the cave entrance, despite the presence of trees in the vicinity and near the edge of the cliff (3.67%; Table S2). They also tend to dissolve easily, especially when burned (Cabanes et al., 2011). Thus, the presence of eudicot leaf phytoliths in such high frequencies indicates that site occupants likely deposited broad leaves of trees or other woody plant forms in large numbers on the mats and beds and that the deposits experienced little disturbance thereafter. Layer Grass Mat 1 and 2 of unit 2 BS.LR C (sample 20), was described as bedding during excavations, as a light brown layer of mixed debris during sampling for phytoliths, and classified in Stratford et al. (2022) as belonging to Facies VII, defined as lightly dispersed anthropogenic units slightly disturbed by trampling or turbation but retaining remnant stratification. This layer is stratigraphically located between the *in situ* bedding layers Grass Mat with bone and Grass Mat 1 b, c (samples 19 and 66) (Fig. 4). No differences in their phytolith assemblages and mixture of minerals were observed. The presence of some calcite in layer Grass Mat 1 and 2 (sample 20) and the location of the major Si–O–Si stretching peak at 1038 cm^{-1} might indicate that this layer was slightly heated, as opposed to that observed in the other two bedding layers (samples 19 and 66), which show the major Si–O–Si stretching peaks are located at 1034 cm^{-1} (SOM 1 – Figure S1). These results show that this layer can also be classified as a bedding layer. Therefore, we might have sampled the edges of the bedding layer, which did not preserve desiccated plant material in the exposed profile sections. Our study thus confirms that using phytoliths together with FTIR, we were able to recognise a bedding layer without the presence of desiccated plant material. High frequencies of articulated phytoliths and fragile morphotypes (i.e. eudicot leaf phytoliths) in relation to unique sets of chemical compounds (e.g. organic matter, gypsum and carbonate hydroxyapatite) and alterations (e.g. exposure to heat) establish robust criteria for identifying bedding deposits with no macroscopically visible preservation of plant material at Border Cave, and potentially other MSA sites. This part of the cave is thus characterised by preserving a continuous succession of beds that are stratigraphically located directly above a hearth (layer Ash, sample 18). The fact that Grass Mat with bone (sample 19) contains some calcite while preserving desiccated plant material (SOM 1 – Figure S1) indicates that coals had already cooled down when plant bedding was placed on top, but some sediment mixing occurred. Yet, it is difficult to assess the temporal relationship between the hearth and the deposition of the grass bedding.

The low variability in the morphology of the eudicot epidermal cells might suggest little species diversity of the leafy material brought to the cave. This correlates well with the macrobotanical remains recovered in bedding layers because only two species of eudicot plants were identified in the 2 WA bedding deposits (Sievers et al., 2022; Backwell et al., 2022). Because charcoal identifications of wood burned at the site reveal a great diversity of eudicot species (Zwane and Bamford, 2021; Lennox et al., 2022), it is plausible that different eudicot species were targeted for different reasons such as making fire, constructing bedding or working mats. We suggest that the leaves of a few specific eudicot species could have been targeted because of their aromatic or healing properties, a practice to maintain clean camps free of pests that started more than 227 ka ago (Wadley et al., 2020a) and became more widely spread in later periods, such as the pre-Still Bay at Sibudu at ~77 ka (Wadley et al., 2011) and the post-HP at Border Cave at ~60 ka.

The bedding layer Dark Brown Dijon from 2 WA.LR (samples 12 and 13) showed a different plant composition with low frequencies of eudicot leaf phytoliths (15.2% and 9.3%, respectively) and the dominance of grasses. Interestingly, Backwell et al. (2022, Fig. 4) report a bed of well-preserved *Chionanthus foveolatus* leaves found in the same layer (Dark Brown Dijon) in the adjacent N118 E109 square. We cannot say that there is a disconnection between plant preservation and phytolith frequencies because we studied different squares and hence plant accumulation could have been different in them. If eudicot leaves were indeed used for bedding in the adjacent square, one would expect their distribution to be confined to a localised area. In this sense, it is plausible that we sampled the edges of Dark Brown Dijon where fewer eudicot leaves were accumulated, explaining the differences observed in the assemblage.

In conclusion, the differences observed in the use of plants to build beds and mats in Border Cave around 60 ka ago could be explained by either a change in human preferences for certain plants or a change in the surrounding plant communities or because the different bedding layers represent living floors that were set aside for specific purposes (e.g. working versus sleeping).

4.2.3. Comparison between the 227,000-year-old and <60,000-year-old bedding features at Border Cave

In the new excavations by Backwell and colleagues, 48 bedding layers have been uncovered throughout the sequence, and they are either desiccated or burned (Backwell et al., 2018, 2022). The grass bedding identified in Member 5 WA and reported by Wadley et al. (2020b), dated to ~227 ka, is represented by siliceous plant fragments. In this study, we compared the phytolith and mineralogical results obtained from Member 5 WA and the post-HP depositional units. We observed that the bedding deposits analysed in this study dating to around 60 ka, differ greatly from the Member 5 WA bedding deposits published in Wadley et al. (2020b) in terms of phytolith concentration and plant composition. Phytolith concentration ranged from 55 to 107 million phytoliths in the 5 WA deposits (Wadley et al., 2020b, Fig. 7a) while in the ~60 ka bedding deposits phytolith concentration ranged from 1.7 to 14.8 million

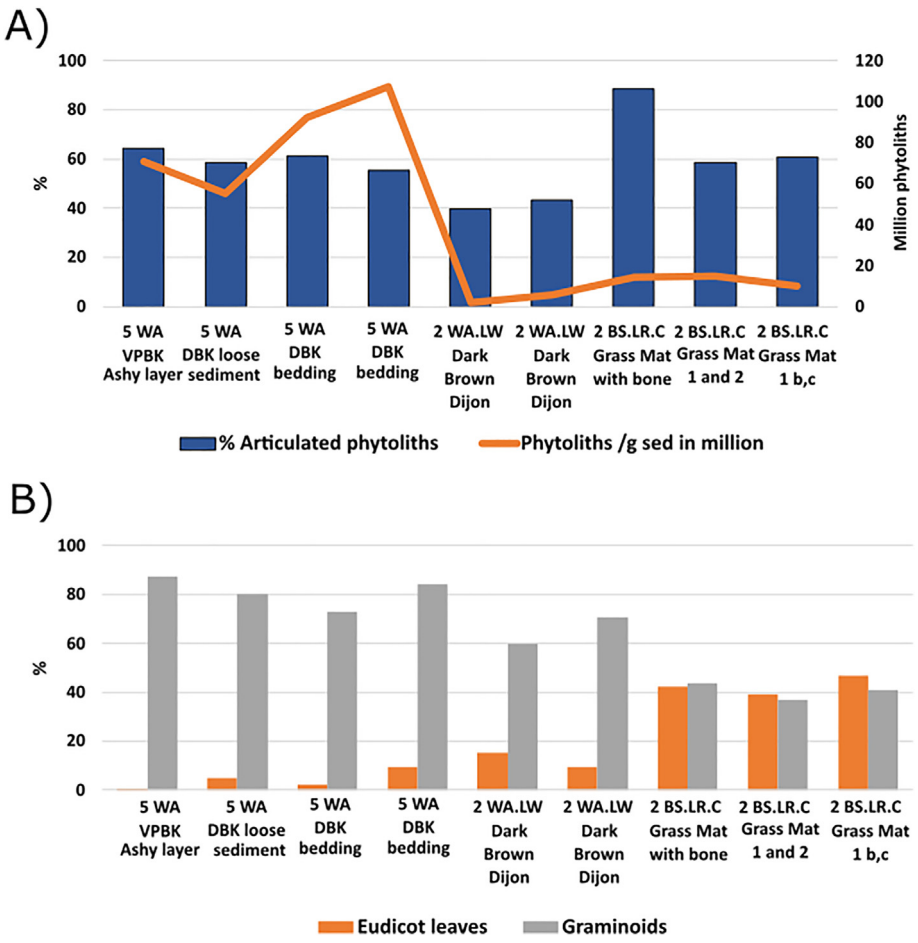

Fig. 7. Comparison of the 2 W A and 2 BS (~60 ka) and 5 W A (~227) bedding layers at Border Cave. A) Distribution of the % of articulated phytoliths and the phytolith concentration (phytoliths per gram of sediment). B) Frequencies of grass and eudicot leaf phytoliths. The % of articulated phytoliths is also plotted for comparison. Layer abbreviations: VPBK= Very Pale Brown Kim, DBK loose = Dark Brown Kent, DBK = Dark Brown Kevin.

phytoliths (Fig. 7a). Conversely, little difference was observed in the % of articulated phytoliths (Fig. 7a). These phytoliths, still in anatomical connection, whether from grasses or tree leaves, were identified at high frequencies in both units. Phytoliths from soils and sediments are not normally recovered in anatomical connection but are instead disarticulated (single cells), and their identification at Border Cave in such high frequencies is indicative of the good state of preservation of the phytolith assemblage. Mineralogically, both member units showed similar mineral composition (see Table 1, and the SOM in Wadley et al., 2020b), with the preservation of chemically unstable minerals such as carbonate hydroxyapatite. These data indicate similar state of preservation of phytolith assemblages in Members 2 WA, 2 BS and 5 WA deposits. However, we cannot rule out the possibility that calcitic ashes (calcite) were part of the original mineral composition of the sediments in Member 5 WA, which could have undergone dissolution with the precipitation of carbonate hydroxyapatite driven by the presence of phosphates (e.g. from food and plant waste) (Schiegl et al., 1996; Weiner et al., 2002). This process could have resulted in a loss of sediment volume and the accumulation (volumetrically) of phytoliths and other less soluble minerals (Schiegl et al., 1996). Sediment compression and loss of volume could also have occurred as part of the combustion process, as was observed through the micromorphological study in the Member 5 WA deposits (Wadley et al., 2020b). The higher densities of lithics in older compared with younger members (Backwell et al., 2022) seem to support this hypothesis. However, this does not entirely explain the differences between the two units. The more time-averaged Member 5 WA deposits, which were accumulated in numerous occupation events (Tribolo et al., 2022), together with the relatively good preservation conditions, as indicated by both the phytoliths and minerals, might also explain the differences observed between the two.

On the other hand, the member units differ in their phytolith morphological composition. Member 5 WA bedding documents a predominance of grass phytoliths, while eudicot leaf phytoliths dominate in most of the Member 2 BS bedding deposits (Fig. 7b). As argued above, it is unlikely that these differences relate to preservation or post-depositional processes. A change in the surrounding environments of Border Cave could be a possibility, which is also supported by the charcoal study that reports dry environments with bushveld and open woodland taxa dominating the record at ~227 ka during the occupation of Member 5 WA (Lennox et al., 2022), conditions that would have favoured the wide availability of grasses. Conversely, moist forests seem to have been the predominant vegetation habitat around Border Cave ~60 ka ago during the occupation of Members 2 BS and 2 WA (Lennox et al., 2022), forests that would have supplied an abundance of eudicot leaves.

In sum, the higher amount of phytoliths in Member 5 WA and differences in phytolith types with respect to members 2 BS and 2 WA do not necessarily indicate a more intensive production of bedding in the older lower member, but rather a change in the plants used for bedding, probably linked to their availability.

5. Conclusions

The phytolith and FTIR study conducted on the complex succession of vertically overlapping deposits of Members 2BS and 2WA has shed further light on the use of plants, pyrotechnology and site occupation patterns at Border Cave ~60 ka ago. Our study demonstrates the importance of combining phytoliths and FTIR to study archaeological deposits at a microscale, and their potential to obtain further information on site formation and post-depositional processes. The identification of bedding deposits with no macroscopically visible preservation of plant material (Layer Grass Mat 1 and 2 of 2 BS.LR C) further proves the applicability of high-resolution analysis combining phytoliths and FTIR to recognise certain behavioural patterns obscured by diagenetic processes or biased during sampling. We also show the ashes of the 2 WA.UP stratified combustion feature in square N109 E118 may have suffered little or no mixing, with the sediment underneath (the reddish and black layers) indicating that this combustion feature is not the result of ash dumping or rake-out.

Indeed, our work also provided empirical support for the ongoing multiscale, multiproxy geoarchaeological research of Stratford et al. (2022). In this sense, we showed that Facies I light brown layers of 2 WA.LR unit are formed primarily by the accumulation of geogenic authigenic minerals, deposits that might represent long periods of slow sediment accumulation during which humans might have visited the site sporadically. Conversely, the results of the light brown layers classified as Facies VI point to a different story, where humans contributed more significantly to the creation of sedimentary deposits. Taphonomic analyses of the kind used here are informative in that they can be used to pinpoint specific layers that might have suffered physical modification, for example in the form of trampling. Our study thus demonstrates that the combination of phytoliths and FTIR are valuable proxies to aid further stratigraphic and facies refinement at Border Cave.

Although grasses and other graminoid- and monocot-associated phytoliths dominate, we observed that the variability observed in our data cannot be explained strictly by differences between types of deposits (combustion features, bedding, and light brown deposits). These variations in the ~60 ka deposits could reflect: (i) different unidentified anthropogenic activities taking place at the site; (ii) different human preferences for certain plants that changed over time; or (iii) changes in the surrounding plant communities. Conversely, the differences we report on the plants used during 5 WA (~227 ka) and 2 BS and 2 WA (~60 ka) bedding layers could be explained by changes in the surrounding environments from a drier environment with bushveld and open woodland taxa around ~227 ka to the dominance of moist forests ~60 ka ago as reported by Lennox et al. (2022).

Finally, it is important to remark that not all the sediment samples from a certain type of deposit or facies showed the same association of phytoliths and minerals. We interpret this evidence as being the result of the nuanced primary or secondary processes taking place at the site during this occupation period, which could not be distinguished at a microscopic scale through the sole application of these two techniques (interpretative equifinality). A micromorphological study of these deposits is thus necessary to help us better understand the origin and depositional and post-depositional histories of the sediments and the complex mineral suite often associated with them (e.g. Karkanas et al., 2000).

Authors contribution

Irene Esteban: Conceptualization, Investigation, Formal analysis, Data Curation, Writing - Original Draft, Visualization; **Dominic Stratford**: Writing - Review & Editing, Funding acquisition; **Christine Sievers**: Writing - Review & Editing; **Paloma de la Peña**: Conceptualization, Writing - Review & Editing; **Guilhem Mauran**: Writing - Review & Editing, Visualization; **Lucinda Backwell**: Border Cave Permit holder and Funder of excavations, Writing - Review & Editing, Visualization; **Francesco d'Errico**: Writing - Review & Editing, Funding acquisition; **Lyn Wadley**: Writing - Review & Editing, Funding acquisition.

Declaration of competing interest

The authors declare that they have no known competing financial interests or personal relationships that could have appeared to influence the work reported in this paper.

Data availability

The data is available as supplementary material

Acknowledgements

IE has received funding from the postdoctoral fellowship programme Beatriu de Pinós (2019 BP00247), funded by the Secretary of Universities and Research (Government of Catalonia) and by the Horizon 2020 programme of research and innovation of the European Union under the Marie Skłodowska-Curie grant agreement No. 801370. Laboratory materials for sample processing at the University of Barcelona were funded by the Ministerio de Ciencia e Innovación - PID 2020-119773 GB-I00. Visit to the site for sampling collection for this study was sponsored by a NRF Y-Rated Research Grant (No. 116358) to DS. PdlP was supported by a Poroulis grant through Cambridge University. PdlP thanks the action PID 2019-1049449 GB-I00 funded by Spanish FEDER/Ministry of Science and Innovation. LB was funded by a National Geographic Explorer grant (NGS-54810R-19), DSI-NRF Centre of Excellence in Palaeosciences (Genus) grant (CEOOP 2020-1), and NRF African Origins Platform grant (No. 98824). Research by FdE is funded by the Research Council of Norway (SFF Centre for Early Sapiens Behaviour-SapienCE-project 262618), the Talents program of the University of Bordeaux (n. 191022_001), and the program "Human Past", funded by the same university. We are grateful to Amafa for issuing us with the excavation permit (SAH 15/7645), and to SAHRA for an export permit (CaseID 15987). We thank two anonymous reviewers for their helpful comments that significantly improved the manuscript.

Appendix A. Supplementary data

Supplementary data to this article can be found online at https://doi.org/10.1016/j.quascirev.2022.107898.

References

Albert, R.M., Cabanes, D., 2007. Fire in prehistory: an experimental approach to combustion processes and phytolith remains. Isr. J. Earth Sci. 56, 175–189.
Anderson, J., 1978. A survey of the extant flora in the vicinity of Border Cave. In: Beaumont, P. (Ed.), Border Cave. M.A. Dissertation. University of Cape Town, pp. 195–213.
Backwell, L., d'errico, F., Banks, W.E., de la Peña, P., Sievers, C., Stratford, D., Lennox, S.J., Wojcieszak, M., Bordy, E.M., Bradfield, J., Wadley, L., 2018. New excavations at Border Cave, KwaZulu-natal, South African. J. Field Archaeol. 43, 417–436.
Backwell, L., Wadley, L., d'Errico, F., Banks, W.E., Peña, P. de la, Stratford, D., Sievers, C., Laue, G., Vilane, B., Clark, J., Tribolo, C., Beaudet, A., Jashashvili, T., Carlson, K.J., Lennox, S., Esteban, I., Mauran, G., 2022. Border Cave: a 227,000-year-old archive from the southern African interior. Quat. Sci. Rev. 291, 107597.
Beaudet, A., d'Errico, Francesco, Backwell, L., Wadley, L., Zipfel, B., de la Peña, P., Reyes-Centeno, H., 2022. A reappraisal of the Border Cave 1 cranium (KwaZulu-Natal, South Africa). Quat. Sci. Rev. 282.
Beaumont, P.B., 1980. On the age of Border Cave hominids 1-5. Palaeontol. Afr. 23,

21–33.
Beaumont, P.B., 1978. Border Cave. (Master's). University of Cape, Town.
Beaumont, P.B., 1973. Border cave- A progress report. S. Afr. Archaeol. Bull. 69, 41–46.
Beaumont, P.B., Miller, G.H., Vogel, J.C., 1992. Contemplating old to the impact of future greenhouse climates in South Africa. South Afr. J. Sci. 88 (9–10).
Beaumont, P.B., Vogel, J.C., 1972. On a new radiocarbon chronology for Africa South of the Equator. Afr. Stud. 31, 65–89.
Bentsen, S.E., 2014. Using pyrotechnology: fire-related features and activities with a focus on the african Middle Stone age. J. Archaeol. Res. 22, 141–175.
Berna, F., Behar, A., Shahack-Gross, R., Berg, J., Boaretto, E., Gilboa, A., Sharon, I., Shalev, S., Shilstein, S., Yahalom-Mack, N., Zorn, J.R., Weiner, S., 2007. Sediments exposed to high temperatures: reconstructing pyrotechnological processes in late bronze and iron age strata at tel dor (Israel). J. Archaeol. Sci. 34, 358–373.
Bird, M.I., Fifield, L.K., Santos, G.M., Beaumont, P.B., Zhou, Y., di Tada, M.L., Hausladen, P.A., 2003. Radiocarbon dating from 40 to 60 ka BP at Border Cave, South Africa. Quat. Sci. Rev. 22, 943–947.
Butzer, K.W., Beaumont, P.B., Vogel, J.C., 1978. Lithostratigraphy of Border Cave, KwaZulu, South Africa: a Middle Stone Age sequence beginning c. 195,000 b. J. Archaeol. Sci. 5, 317–341.
Cabanes, D., Mallol, C., Expósito, I., Baena, J., 2010. Phytolith evidence for hearths and beds in the late Mousterian occupations of Esquilleu cave (Cantabria, Spain). J. Archaeol. Sci. 37, 2947–2957.
Cabanes, D., Weiner, S., Shahack-Gross, R., 2011. Stability of phytoliths in the archaeological record: a dissolution study of modern and fossil phytoliths. J. Archaeol. Sci. 38, 2480–2490.
Chukanov, N.V., Vigasina, M.F., 2020. Vibrational (Infrared and Raman) Spectra of Minerals and Related Compounds. Springer Nature Switzerland AG.
Conard, N.J., Porraz, G., Wadley, L., 2012. What is in a name?: characterising the "post-howieson's Poort" at Sibudu. South african archaeol. Bull. (Arch. Am. Art) 67, 180–199.
de la Peña, P., Colino, F., d'Errico, Francesco, Wadley, L., Banks, W.E., Stratford, D., Backwell, L., 2022. Lithic technological and spatial analysis of the final Pleistocene at Border Cave, South Africa. Quat. Sci. Rev. 296, 107802.
de Vynck, J.C., van Wyk, B.-E., Cowling, R.M., 2016. Indigenous edible plant use by contemporary Khoe-San descendants of South Africa's Cape South Coast. South Afr. J. Bot. 102, 60–69.
Deacon, H.J., 1993. Planting an idea: an archaeology of Stone age gatherers in South Africa. South african archaeol. Bull. (Arch. Am. Art) 48, 86.
Cooke, H.B.S., Malan, B.D., Wells, L.H., et al., 1945. Fossil man in the Lebombo mmountains, South Africa: the 'Border Cave,' Ingwavuma district, Zululand. Man 45 (3), 6–13.
d'Errico, F., Backwell, L., 2016. Earliest evidence of personal ornaments associated with burial: the Conus shells from Border Cave. J. Hum. Evol. 93, 91–108.
d'Errico, F., Backwell, L., Villa, P., Degano, I., Lucejko, J.J., Bamford, M.K., Higham, T.F.G., Colombini, M.P., Beaumont, P.B., 2012. Early evidence of San material culture represented by organic artifacts from Border Cave, South Africa. P. Natl. Acad. Sci. USA 109, 13214–13219.
Dusseldorp, G.L., 2014. Explaining the Howiesons Poort to post-Howiesons Poort transition: a review of demographic and foraging adaptation models. Azania 49, 317–353.
Eichhorn, B., Neumann, K., Garnier, A., 2010. Seed phytoliths in West African Commelinaceae and their potential for palaeoecological studies. Palaeogeogr. Palaeoclimatol. Palaeoecol. 298, 300–310.
Esteban, I., 2016. Reconstructing Past Vegetation and Modern Human Foraging Strategies on the South Coast of South Africa (PhD). Universitat de Barcelona.
Esteban, I., de Vynck, J.C., Singels, E., Vlok, J.H.J., Marean, C.W., Cowling, R.M., Fisher, E.C., Cabanes, D., Albert, R.M., 2017a. Modern soil phytolith assemblages used as proxies for Paleoscape reconstruction on the south coast of South Africa. Quat. Int. 434, 160–179.
Esteban, I., Fitchett, J.M., de la Peña, P., 2020. Plant taphonomy, flora exploitation and palaeoenvironments at the Middle Stone Age site of Mwulu ' s Cave (Limpopo, South Africa): an archaeobotanical and mineralogical approach. Archaeol. Anthropol. Sci. 12 (226), 1–18.
Esteban, I., Marean, C.W., Fisher, E.C., Karkanas, P., Cabanes, D., Albert, R.M., 2018. Phytoliths as an indicator of early modern humans plant gathering strategies, fire fuel and site occupation intensity during the Middle Stone Age at Pinnacle Point 5-6 (south coast, South Africa). PLoS One 13, e0198558.
Esteban, I., Vlok, J.H.J., Kotina, E.L., Bamford, M.K., Cowling, R.M., Cabanes, D., Albert, R.M., 2017b. Phytoliths in plants from the south coast of the greater cape floristic region (South Africa). Rev. Palaeobot. Palynol. 245, 69–84.
Gebashe, F., Moyo, M., Aremu, A.O., Finnie, J.F., van Staden, J., 2019. Ethnobotanical survey and antibacterial screening of medicinal grasses in KwaZulu-Natal Province, South Africa. South Afr. J. Bot. 122, 467–474.
Geiger, S.B., Weiner, S., 1993. Fluoridated carbonatoapatite in the intermediate layer between glass ionomer and dentin. Dent. Mater. 9, 33–36.
Goldberg, P., Miller, C.E., Schiegl, S., Ligouis, B., Berna, F., Conard, N.J., Wadley, L., 2009. Bedding, hearths, and site maintenance in the Middle Stone age of Sibudu cave, KwaZulu-natal, South Africa. Archaeol. Anthropol. Sci. 1, 95–122.
Grün, R., Beaumont, P., 2001. Border Cave revisited: a revised ESR chronology. J. Hum. Evol. 40, 467–482.
Grün, R., Beaumont, P., Tobias, P.v., Eggins, S., 2003. On the age of Border Cave 5 human mandible. J. Hum. Evol. 45, 155–167.
Karkanas, P., Bar-Yosef, O., Goldberg, P., Weiner, S., 2000. Diagenesis in prehistoric caves: the use of minerals that form in situ to assess the completeness of the archaeological record. J. Archaeol. Sci. 27, 915–929.
Karkanas, P., Goldberg, P., 2010. Phosphatic features. In: Interpretation of Micromorphological Features of Soils and Regoliths. Elsevier, pp. 521–541.
Katz, O., Cabanes, D., Weiner, S., Maeir, A.M., Boaretto, E., Shahack-Gross, R., 2010. Rapid phytolith extraction for analysis of phytolith concentrations and assemblages during an excavation: an application at Tell es-Safi/Gath, Israel. J. Archaeol. Sci. 37, 1557–1563.
Lennox, S., Backwell, L., d'Errico, F., Wadley, L., 2022. A vegetation record based on charcoal analysis from Border Cave, KwaZulu-Natal, South Africa, ~227 000 to ~44 000 years ago. Quat. Sci. Rev. 293, 107676.
Lippmann, F., 1973. Sedimentary Carbonate Minerals. Springer-Verlag, New York.
Lombard, M., Parsons, I., 2011. What happened to the human mind after the Howiesons Poort? Antiq 85, 1433–1443.
Mackay, A., Stewart, B.A., Chase, B.M., 2014. Coalescence and fragmentation in the late Pleistocene archaeology of southernmost Africa. J. Hum. Evol. 72, 26–51.
Mallol, C., Hernández, C.M., Cabanes, D., Sistiaga, A., Machado, J., Rodríguez, Á., Pérez, L., Galván, B., 2013. The black layer of Middle Palaeolithic combustion structures. Interpretation and archaeostratigraphic implications. J. Archaeol. Sci. 40, 2515–2537.
Mayori, A., 2017. Diversity of use and local knowledge of wild and cultivated plants in the Eastern Cape province, South Africa. J. Ethnobiol. Ethnomed. 13.
McCall, G.S., 2007. Behavioral ecological models of lithic technological change during the later Middle Stone Age of South Africa. J. Archaeol. Sci. 34, 1738–1751.
Millard, A.R., 2006. Bayesian analysis of ESR dates, with application to Border Cave. Quat. Geochronol. 1, 159–166.
Miller, C., Conard, N., Goldberg, P., Berna, F., 2010. Dumping, sweeping and trampling: experimental micromorphological analysis of anthropogenically modified combustion features. Faculty of Science (Medicine and Health - Papers: part A).
Miller, G.H., Beaumont, P.B., Deacon, H.J., Brooks, A.S., Hare, P.E., Jull, A.J.T., 1999. Earliest modern humans in southern Africa dated by isoleucine epimerization in ostrich eggshell. Quat. Sci. Rev. 18, 1537–1548.
Mogale, M.M.P., Raimondo, D.C., VanWyk, B.E., 2019. The ethnobotany of central sekhukhuneland, South Africa. South Afr. J. Bot. 122, 90–119.
Murungi, M.L., 2017. Phytoliths at Sibudu (South Africa): Implications for Vegetation, Climate and Human Occupation during the MSA (PhD). University of the Witwatersrand.
Neumann, Katharina, Strömberg, Caroline, Ball, Terry, Albert, Rosa Maria, Vrydaghs, Luc, Cummings, Linda Scott, et al., International Committee for Phytolith Taxonomy (ICPT), 2019. International code for phytolith nomenclature (ICPN) 2.0. Annals of Botany 124 (2), 189–199.
Nortje, J.M., van Wyk, B.E., 2019. Useful plants of Namaqualand, South Africa: a checklist and analysis. South Afr. J. Bot. 122, 120–135.
Piperno, D.R., 2006. Phytoliths: a Comprehensive Guide for Archaeologists and Paleoecologists. AltaMira Press, Lanham, MD.
Ramsey, M.N., Maher, L.A., Macdonald, D.A., Nadel, D., Rosen, A.M., 2018. Sheltered by reeds and settled on sedges: construction and use of a twenty thousand-year-old hut according to phytolith analysis from Kharaneh IV, Jordan. J. Anthropol. Archaeol. 50, 85–97.
Regev, L., Poduska, K.M., Addadi, L., Weiner, S., Boaretto, E., 2010. Distinguishing between calcites formed by different mechanisms using infrared spectrometry: archaeological applications. J. Archaeol. Sci. 37, 3022–3029.
Riley, T.R., Millar, I.L., Watkeys, M.K., Curtis, M.L., Leat, P.T., Klausen, M.B., Fanning, C.M., 2004. U–Pb zircon (SHRIMP) ages for the Lebombo rhyolites, South Africa: refining the duration of Karoo volcanism. J. Geol. Soc. London 161, 547–550.
Rutherford, M.C., Mucina, L., Lötter, M.C., Bredenkamp, G.J., Smit, J.H.L., Scott-Shaw, C.R., Hoare, D.B., Goodman, P.S., Bezuidenhout, H., Scott, L., Ellis, F., Powrie, L.W., Siebert, F., Mostert, T.H., Henning, B.J., Venter, C.E., Camp, K., Siebert, S.J., Matthews, W.S., Burrows, J.E., Dobson, L., Rooyen, N. van, Schmidt, E., Winter, P.J.D., Preez, P.J. du, Robert, A., Ward, S., Williamson, A., Hurter, P.J.H., 2006. Savanna biome. In: Mucina, L., Rutherford, M. (Eds.), The Vegetation of South Africa, Lesotho and Swaziland. South African National Biodiversity Institute, pp. 429–529.
Scaillet, B., Macdonald, R., 2004. Fluorite stability in silicic magmas. Contrib. Mineral. Petrol. 147 (3), 319–329.
Schiegl, S., Conard, N.J., 2006. The Middle Stone Age sediments at Sibudu: results from FTIR spectroscopy and microscopic analyses. South. African Humanit. 18, 149–172.
Schiegl, S., Goldberg, P., Bar-Yosef, O., Weiner, S., 1996. Ash deposits in Hayonim and Kebara caves, Israel: macroscopic, microscopic and mineralogical observations, and their archaeological implications. J. Archaeol. Sci. 23, 763–781.
Schiegl, S., Stockhammer, P., Scott, C., Wadley, L., 2004. A mineralogical and phytolith study of the Middle Stone age hearths in Sibudu cave, KwaZulu-natal, South Africa: Sibudu cave. S. Afr. J. Sci. 100, 185–194.
Shackleton, C., Sinasson, G., Adeyemi, O., Martins, V., 2022. Fuelwood in South Africa revisited: widespread use in a policy vacuum, 2022 Sustainability 14, 11018 14, 11018.
Shahack-Gross, R., Berna, F., Karkanas, P., Weiner, S., 2004. Bat guano and preservation of archaeological remains in cave sites. J. Archaeol. Sci. 31, 1259–1272.
Sievers, C., Backwell, L., d'Errico, Francesco, Wadley, L., 2022. Plant bedding construction between 60,000 and 40,000 years ago at Border Cave, South Africa. Quat. Sci. Rev. 275, 107280.
Stratford, D., Clark, J.L., Wojcieszak, M., Wadley, L., d'Errico, F., de la Peña, P.,

Esteban, I., Sievers, C., Banks, W.E., Beard, T., Horn, M., Shadrach, K., Morrissey, P., Mauran, G., Backwell, L., 2022. Geoarchaeology and zooarchaeology of Border Cave, South Africa: initial multiproxy considerations of stratigraphy and site formation processes from the Backwell et al. excavations. Quat. Sci. Rev. 291, 107618.
Timbrell, L., de la Peña, P., Way, A., Hoggard, C., Backwell, L., d'Errico, F., Wadley, L., Grove, M., 2022. Technological and geometric morphometric analysis of 'post-Howiesons Poort points' from Border Cave, KwaZulu-Natal, South Africa. Quat. Sci. Rev. 297, 107813.
Toffolo, M.B., Brink, J.S., Berna, F., 2015. Bone diagenesis at the florisbad spring site, free state province (South Africa): implications for the taphonomy of the Middle and late pleistocene faunal assemblages. J. Archaeol. Sci. Rep. 4, 152–163.
Tribolo, C., Mercier, N., Dumottay, C., Cantin, N., Banks, W.E., Stratford, D., Peña de la, P., Backwell, L., Wadley, L., d'Errico, Francesco, 2022. Luminescence dating at Border Cave: attempts, questions, and new results. Quat. Sci. Rev. 296, 107787.
van Wyk, B.E., 2008. A review of Khoi-San and Cape Dutch medical ethnobotany. J. Ethnopharmacol.
van Wyk, B.-E., Gericke, N., 2000. People's Plants: a Guide to Useful Plants of Southern Africa. Briza Publications, Johannesburg.
Villa, P., Delagnes, A., Wadley, L., 2005. A late Middle Stone age artifact assemblage from Sibudu (KwaZulu-Natal): comparisons with the European Middle paleolithic. J. Archaeol. Sci. 32, 399–422.
Villa, P., Soriano, S., Tsanova, T., Degano, I., Higham, T.F.G., D'Errico, F., Backwell, L., Lucejko, J.J., Colombini, M.P., Beaumont, P.B., 2012a. Border cave and the beginning of the later Stone age in South Africa. P. Natl. Acad. Sci. USA 109, 13208–13213.
Villa, P., Soriano, S., Tsanova, T., Degano, I., Higham, T.F.G., d'Errico, F., Backwell, L., Lucejko, J.J., Colombini, M.P., Beaumont, P.B., 2012b. Border cave and the beginning of the later Stone age in South Africa. P. Natl. Acad. Sci. USA 109, 13208–13213.
Vogel, J.C., Beaumont, P.B., 1972. Revised radiocarbon chronology for the Stone age in South Africa. Nature 237, 50–51.
Vogel, J.C., Fuls, A., Visser, E., 1986. Pretoria radiocarbon dates III. Radiocarbon 28, 1133–1172.
Wadley, L., 2015. Those marvellous millennia: the Middle Stone age of southern Africa. Azania 50, 155–226.
Wadley, L., 2012. Some combustion features at Sibudu, South Africa, between 65,000 and 58,000 years ago. Quat. Int. 247, 341–349.
Wadley, L., Sievers, C., Bamford, M.K., Goldberg, P., Berna, F., Miller, C., 2011. Middle Stone Age bedding construction and settlement patterns at Sibudu, South Africa. Science 334, 1388–1391, 1979.
Wadley, L., Backwell, L., d'errico, F., Sievers, C., 2020a. Cooked starchy rhizomes in Africa 170 thousand years ago. Science 367, 87–91.
Wadley, L., Esteban, I., de la Peña, P., Wojcieszak, M., Stratford, D., Lennox, S., d'Errico, F., Rosso, D.E., Orange, F., Backwell, L., Sievers, C., 2020b. Fire and grass-bedding construction 200 thousand years ago at Border Cave, South Africa. Science 369, 863–866.
Weiner, S., 2010. Microarchaeology. Beyond the Visible Archaeological Record. Cambridge University Press.
Weiner, S., Goldberg, P., Bar-Yosef, O., 2002. Three-dimensional distribution of minerals in the sediments of Hayonim Cave, Israel: diagenetic processes and archaeological implications. J. Archaeol. Sci. 29, 1289–1308.
Weinstein-Evron, M., Tsatskin, A., Weiner, S., Shahack-Gross, R., Frumkin, A., Yeshurun, R., Zaidner, Y., 2012. A window into early Middle paleolithic human occupational layers: misliya cave, mount carmel, Israel. PaleoAnthropology 202–228.
Wiessner, P.W., 2014. Embers of society: firelight talk among the Ju/'hoansi Bushmen. P. Natl. Acad. Sci. USA 111, 14027–14035.
Will, M., 2019. Sibudan. In: Chirikure, S. (Ed.), Oxford Research Encyclopedia of Anthropology. Oxford University Press, New York.
Zwane, B., Bamford, M., 2021. Wood charcoal from Border Cave's member 1RGBS: evidence for the environment and plant use during MIS 5. Afr. Archaeol. Rev. 38, 657–674.